NISTIR 6053

Electronics and Electrical Engineering Laboratory

J. M. Rohrbaugh
Compiler

Technical Progress Bulletin

97-2

Covering Laboratory Programs,
April to June 1997,
with 1997-1998 EEEL Events Calendar

U.S. DEPARTMENT OF COMMERCE
Technology Administration
National Institute of Standards
and Technology

NIST

NISTIR 6053

Electronics and Electrical Engineering Laboratory

J. M. Rohrbaugh
Compiler

Electronics and Electrical
Engineering Laboratory
Semiconductor Electronics Division
Gaithersburg, MD 20899-0001

Technical Progress Bulletin

September 1997

97-2

Covering Laboratory Programs,
April to June 1997,
with 1997-1998 EEEL Events Calendar

U.S. DEPARTMENT OF COMMERCE
William M. Daley, Secretary
TECHNOLOGY ADMINISTRATION
Gary Bachula, Acting Under Secretary
for Technology
NATIONAL INSTITUTE OF STANDARDS
AND TECHNOLOGY
Robert E. Hebner, Acting Director

ELECTRONICS AND ELECTRICAL ENGINEERING LABORATORY
TECHNICAL PROGRESS BULLETIN, SEPTEMBER 1997 ISSUE

INTRODUCTION

This is the fifty-seventh issue of a publication providing information on the technical work of the National Institute of Standards and Technology Electronics and Electrical Engineering Laboratory (EEEL). This issue of the EEEL Technical Progress Bulletin covers the second quarter of calendar year 1997.

Organization of Bulletin: This issue contains abstracts for all relevant papers released for publication by NIST in the quarter and citations and abstracts for such papers published in the quarter. Entries are arranged by technical topic as identified in the Table of Contents and alphabetically by first author under each subheading within each topic. Unpublished papers appear under the subheading "Released for Publication." This does not imply acceptance by any outside organization. Papers published in the quarter appear under the subheading "Recently Published." Following each abstract is the name and telephone number of the individual to contact for more information on the topic (usually the first author). This issue also includes a calendar of Laboratory conferences and workshops planned for calendar years 1997 through 1998 and a list of sponsors of the work.

Electronics and Electrical Engineering Laboratory: EEEL programs provide national reference standards, measurement methods, supporting theory and data, and traceability to national standards. The metrological products of these programs aid economic growth by promoting equity and efficiency in the marketplace, by removing metrological barriers to improved productivity and innovation, by increasing U.S. competitiveness in international markets through facilitation of compliance with international agreements, and by providing technical bases for the development of voluntary standards for domestic and international trade. These metrological products also aid in the development of rational regulatory policy and promote efficient functioning of technical programs of the Government.

The work of the Laboratory is conducted by five technical research Divisions: the Semiconductor Electronics and the Electricity Divisions in Gaithersburg, Md., and the Electromagnetic Fields, Electromagnetic Technology, and the Optoelectronics Divisions in Boulder, Colo. The Office of Law Enforcement Standards conducts research and provides technical services to the U.S. Department of Justice and State and local governments, and other agencies in support of law enforcement activities. In addition, the Office of Microelectronics Programs (OMP) coordinates the growing number of semiconductor-related research activities at NIST. Reports of EEEL work funded through the OMP are included under the heading "Semiconductor Microelectronics."

Key contacts in the Laboratory are listed at the end of this publication; readers are encouraged to contact any of these individuals for further information. To request a subscription or for more information on the Bulletin, write to EEEL Technical Progress Bulletin, National Institute of Standards and Technology, Metrology Building, Room B-358, Gaithersburg, MD 20899 or call (301) 975-2220.

Laboratory Sponsors: The Laboratory Programs are sponsored by the National Institute of Standards and Technology and a number of other organizations, in both the Federal and private sectors; these are identified on page 32.

Note on Publication Lists: Publication lists covering the work of each division are guides to earlier as well as recent work. These lists are revised and reissued on an approximately annual basis and are available from the originating division. The current set is identified in the Additional Information section, page 30.

Certain commercial equipment, instruments, or materials are identified in this paper in order to specify adequately the experimental procedures. Such identification does not imply recommendation or endorsement by the National Institute of Standards and Technology, nor does it imply that the materials or equipment identified are necessarily the best available for the purpose.

Internet Access (World Wide Web): http://www.eeel.nist.gov

TO LEARN MORE ABOUT THE LABORATORY...

Two general documents are available that may be of interest. These are ***EEEL 1996 Technical Accomplishments, Advancing Metrology for Electrotechnology to Support the U.S. Economy*** and ***Measurements for Competitiveness in Electronics***. The first presents selected technical accomplishments of the Laboratory for the period October 1, 1995 through September 30, 1996. A brief indication of the nature of the technical achievement and the rationale for its undertaking are given for each example. The second identifies measurement needs for a number of technical areas and the general importance of measurements to competitiveness issues. The findings of each chapter dealing with an individual industry have been reviewed by members of that industry. A longer description of both documents follows:

EEEL 1996 Technical Accomplishments, Advancing Metrology for Electrotechnology to Support the U.S. Economy, NISTIR 5941 (December 1996).

The Electronics and Electrical Engineering Laboratory, working in concert with other NIST Laboratories, is providing measurement and other generic technology critical to the competitiveness of the U.S. electronics industry and the U.S. electricity-equipment industry. This report summarizes selected technical accomplishments and describes activities conducted by the Laboratory in FY 1996 in the field of semiconductors, magnetics, superconductors, low-frequency microwaves, lasers, optical fiber communications and sensors, video, power, electromagnetic compatibility, electronic data exchange, and national electrical standards. Also included is a profile of EEEL's organization, its customers, and the Laboratory's long-term goals.

EEEL is comprised of five technical divisions, Electricity and Semiconductor Electronics in Gaithersburg, Maryland, and Electromagnetic Fields, Electromagnetic Technology, and Optoelectronics in Boulder, Colorado. Through two offices, the Laboratory manages NIST-wide programs in microelectronics and law enforcement.
[Contact: JoAnne Surette, (301) 975-5267]

Measurements for Competitiveness in Electronics, NISTIR 4583 (April 1993).

Measurements for Competitiveness in Electronics identifies for selected technical areas the measurement needs that are most critical to U.S. competitiveness, that would have the highest economic impact if met, and that are the most difficult for the broad range of individual companies to address. The document has two primary purposes: (1) to show the close relationship between U.S. measurement infrastructure and U.S. competitiveness and show why improved measurement capability offers such high economic leverage, and (2) to provide a statement of the principal measurement needs affecting U.S. competitiveness for given technical areas, as the basis for a possible plan to meet those needs, should a decision be made to pursue this course.

The first three chapters, introductory in nature, cover the areas of: the role of measurements in competitiveness, NIST's role in measurements, and an overview of U.S. electronics and electrical-equipment industries. The remaining nine chapters address individual fields of electronic technology: semiconductors, magnetics, superconductors, microwaves, lasers, optical-fiber communications, optical-fiber sensors, video, and electromagnetic compatibility. Each of these nine chapters contains four basic types of information: technology review, world markets and U.S. competitiveness, goals of U.S. industry for competitiveness, and measurement needs. Three appendices provide definitions of the U.S. electronics and electrical-equipment industries.
[Contact: Ronald M. Powell, (301) 975-2220]

FitzPatrick, G.J., Olthoff, J.K., and Powell, R.M., **Measurement Support for the U.S. Electric-Power Industry in the Era of Deregulation with Focus on Electrical Measurements for Transmission and Distribution**, NISTIR 6007 (May 1997).

The U.S. electric-power industry, comprising the generation, transmission, and distribution systems throughout the country, has been described as the "greatest machine ever created." This machine is an integral part of the national infrastructure. Its continued good performance is vital to the success of the economy, to the pursuit of environmental and health goals, and to the assurance of safety and security.

Dramatic changes are now taking place in the U.S. electric-power industry as deregulation is implemented and as competition is introduced in providing electric power. These changes offer the possibility of lower prices for electric power and increased supply, with minimal increases in associated capital facilities. To achieve these goals in a competitive environment, the industry will have to exploit fully the capabilities of modern technology. To succeed in such exploitation, the industry will require new measurement capability.

This document describes the changes taking place in the industry. These changes are translated into technical needs associated with industry's response and then into the associated measurement needs for which the assistance of the National Institute of Standards and Technology (NIST) will be required. The resulting measurement needs are grouped into categories by priority. The highest priority needs are generally those with the greatest prospective economic impact.

This document focuses principally on measurement capability for the *electrical quantities* associated with the *transmission and distribution* of electric power. Special emphasis is placed on those measurement needs requiring the assistance of NIST. There are also important measurement needs associated with the efficient generation and use of electricity. They are the subject of other inquiries now underway at NIST.

The assessment presented here reflects NIST's current understanding of the key measurement needs, based on interactions with industry, universities, and government during the development of this document. Through publication of this document, NIST solicits additional feedback on the measurement needs of this industry. NIST's purpose is to assure that its resources are applied as effectively as possible in support of the U.S. electric-power industry and its customers nationwide.

Copies of this document are available as Order No. PB97-152508 from the National Technical Information Service, 5285 Port Royal Road, Springfield, Virginia 22161, at (800) 553-6847 or at (703) 487-4650. Order may also be placed by fax at (703) 321-8547 or by electronic mail at orders@ntis.fedworld.gov.
[Contact: Gerald J. FitzPatrick, (303) 975-2737]

TABLE OF CONTENTS

GENERAL INFORMATION

Released for Publication

Oldham, N.M., **Importance of Standards and Traceability in the Power Industry**, to be published in the Proceedings of the Primer Simposio Sobre Mediciones en Comision Federal de Electricidad, Mexico City, Mexico, April 17, 1997.

Standards associated with the power industry not only influence the sale of electric energy, but also the way electrical equipment is manufactured, tested, and sold in the global market. The structure of international and regional standards organizations is explained, and the American National Standards Institute C12.1 "Code for Electricity Metering," is described in detail.
[Contact: Nile M. Oldham, (301) 975-2408]

FUNDAMENTAL ELECTRICAL MEASUREMENTS

Released for Publication

Benz, S.P., Hamilton, C.A., Burroughs, C.J., and Christian, L.A., **Josephson Standards for AC Voltage Metrology**, to be published in the Proceedings of the 1997 National Conference of Standards Laboratories, Atlanta, Georgia, July 27-31, 1997.

We have designed a new generation Josephson array that replaces the traditional superconductor-insulator-superconductor junctions with superconductor-normal metal-superconductor (SNS) junctions. These new arrays generate inherently stable voltages and respond to broadband inputs that can be programmed to generate metrologically accurate ac waveforms. To do this, we use an input to an SNS junction arrays that consists of a long (up to 8 Mbits), repetitive, digital pulse train that is clocked at frequencies up to 12 Gbit/s. In preliminary experiments using arrays of 1000 junctions, this technique has been used to synthesize both stable dc levels and sinewaves of a few millivolts in amplitude at frequencies up to 1 MHz. The continuing effort is focused on increasing the clock frequency and the number of junctions in the array to achieve metrologically practical voltages of a few volts.
[Contact: Samuel P. Benz, (303) 497-5258]

Benz, S.P., Hamilton, C.A., Burroughs, C.J., Christian, L.A., and Przybysz, J.X., **A Pulse-Driven Josephson Digital/Analog Converter**, to be published in the Proceedings of the 1997 International Superconductive Electronics Conference, Berlin, Germany, June 25-28, 1997.

We have designed and demonstrated a pulse-driven Josephson digital/analog converter. When used as a programmable voltage standard, this device can synthesize metrologically accurate ac waveforms, as well as stable dc voltages. We show through simulations that Josephson quantization produces a nearly ideal quantization noise spectrum when a junction is driven with a typical waveform produced by a digital code generator. This technique has been demonstrated in preliminary experiments with arrays of 1000 junctions clocked at frequencies up to 12 Gbit/s where sine waves of a few millivolts in amplitude were synthesized at frequencies up to 1 MHz.
[Contact: Samuel P. Benz, (303) 497-5258]

Benz, S.P., Hamilton, C.A., Burroughs, C.J., Harvey, T.E., and Christian, L.A., **Stable 1-Volt Programmable Voltage Standard**.

Several fully functional programmable voltage standard chips, each having a total of 32,768 Nb-PdAu-Nb Josephson junctions, have been fabricated and tested. The chips are based on a new design that provides fast programmability (1 μs) between voltages and stable voltage operation from -1 V to +1 V. A comparison of the new standard with a conventional Josephson voltage standard is in agreement to 0.5 ± 1.1 parts in 10^9. We demonstrate the utility of this new standard by measuring the linearity of a digital voltmeter.
[Contact: Samuel P. Benz, (303) 497-5258]

Cage, M.E., **Current Distributions in Quantum Hall Effect Devices**, to be published in Journal of Research of the National Institute of Standards and Technology.

This paper addresses the question of how current is distributed within quantum Hall effect devices. Three types of flow patterns most often mentioned in the literature are considered. They are skipping

orbits along the device periphery (which arise from elastic collisions off hard-walled potentials), narrow conducting channels along the device sides (which are presumed to be generated from confining potentials), and currents distributed throughout the device (which are assumed to arise from a combination of confining and charge-redistribution potentials). The major conclusions are that skipping orbits do not occur in quantum Hall effect devices, and that nearly all of the externally applied current is located within the device interior rather than along the device edges.
[Contact: Marvin E. Cage, (301) 975-4224]

FUNDAMENTAL ELECTRICAL MEASUREMENTS

Recently Published

Benz, S.P., and Burroughs, C.J., **Constant-Voltage Steps in Arrays of Nb-PdAu-Nb Josephson Junctions**, IEEE Transactions on Applied Superconductivity, Vol. 7, No. 2, pp. 2434-2437 (June 1997).

Design and fabrication of Nb-PdAu-Nb trilayer Josephson junctions are described. The microwave response of an array of 1000 of these junctions was measured, and constant-voltage step heights were characterized as a function of the microwave amplitude and frequency. Experimental results fit well to point-junction simulations at the 3 GHz design frequency of the microwave distribution network. The observed step height of 3.8 mA shows that the array and microwave distribution are sufficiently uniform for application in programmable Josephson voltage standards.
[Contact: Samuel P. Benz, (303) 497-5258]

Benz, S.P., Burroughs, C.J., and Hamilton, C.A., **Operating Margins for a Pulse-Driven Programmable Voltage Standard**, IEEE Transactions on Applied Superconductivity, Vol. 7, No. 2, pp. 2653-2656 (June 1997).

We have designed and fabricated a Josephson voltage standard where the voltage can be rapidly and continuously programmed by changing the repetition frequency of a pulse drive. Simulations are made to optimize the operating margins of the circuit for different pulse waveforms. The response of a 1000-junction array of Nb-PdAu-Nb junctions is measured, and constant-voltage step heights are characterized as a function of the pulse amplitude, pulse width, and frequency. A dc bias range of 0.62 mA is demonstrated over a continuous voltage-tunable range from -6.2 mV to +6.5 mV.
[Contact: Samuel P. Benz, (303) 497-5258]

Hamilton, C.A., Benz, S.P., Burroughs, C.J., and Harvey, T.E., **SNS Programmable Voltage Standard**, IEEE Transactions on Applied Superconductivity, Vol. 7, No. 2, pp. 2472-2475 (June 1997).

Superconductor-Normal-Superconductor (SNS) junctions have been used in the design and fabrication of a 1 V rapidly programmable voltage standard. The superconducting circuit is a series array of 32 768 Nb-PdAu-Nb junctions with taps that divide the array into a binary sequence of smaller array segments with a minimum segment size of 128 junctions. The 16 GHz drive frequency is set by the characteristic frequency of the junctions. A computer-controlled eight-channel bias system controls the current in each segment and allows the rapid selection of any one of 513 discrete voltage levels. The system is designed for fast dc measurements and the synthesis of precise ac waveforms.
[Contact: Clark A. Hamilton, (303) 497-3740]

Hamilton, C.A., Buroughs, C.J., Kupferman, S.L., Naujoks, G.A., and Vickery A., **A Compact Transportable Josephson Voltage Standard**, IEEE Transactions on Instrumentation and Measurement, Vol. 46, No. 2, pp. 237-241 (April 1997).

The development of a compact, portable 10 V Josephson calibration system is described. Its accuracy is the same as typical laboratory systems, but its weight and volume are reduced by more than a factor of three. The new system will replace conventional travelling voltage standards used within several NASA and DOE standards laboratories.
[Contact: Clark A. Hamilton, (303) 497-3740]

Hamilton, C.A., Burroughs, C.J., and Benz, S.P., **Josephson Voltage Standard - A Review**, IEEE Transactions on Applied Superconductivity, Vol. 7, No. 2, pp. 3756-3761 (June 1997).

The unique ability of a Josephson junction to convert a microwave frequency *f* into a voltage *Nhf/2e* with high accuracy and the adoption of this phenomenon as the basis for the SI Volt Realization have created a market for Josephson voltage standards that is unassailable from any other technology. This paper reviews the development of Josephson voltage standards including the junction and array design, the microwave circuit, and the system integration. With the dc Josephson standard largely transferred to the commercial sector, NIST is developing a new class of devices in which the output voltage can be rapidly programmed either by digitally selecting the quantum number *N* or by driving the Josephson array with a variable frequency pulse train. These new devices will make possible fast, high-accuracy characterizations of A/D and D/A converters and the synthesis of ac waveforms.
[Contact: Clark A. Hamilton, (303) 497-3740]

Keller, M.W., Martinis, J.M., Steinbach, A.H., and Zimmerman, N.M., **A Seven-Junction Electron Pump: Design, Fabrication, and Operation**, IEEE Transactions on Instrumentation and Measurement, Vol. 46, No. 2, pp. 307-310 (April 1997).

We have developed a seven-junction electron pump for use in a new standard of capacitance based on measuring the voltage produced when a known charge is placed on a capacitor. This new pump, with an error per pumped electron of 15×10^{-9}, is about 30 times more accurate than a five-junction pump made previously at NIST. By careful design of the pump geometry, we have reduced the effect of cross capacitance and simplified device operation. Our fabrication recipe produces small, stable tunnel junctions relatively quickly and reliably. We have developed a method of tuning the pump for highly accurate electron counting. This tuning can be quickly repeated whenever fluctuations in background charges degrade accuracy.
[Contact: John M. Martinis, (303) 497-3597]

SEMICONDUCTOR MICROELECTRONICS

Compound Materials

Recently Published

Talwar, D.N., Roughani, B., Pellegrino, J.G., Amirtharaj, P.M., and Qadri, S.B., **Study of Phonons in Semiconductor Superlattices by Raman Scattering Spectroscopy and Microscopic Model Calculation**, Materials Science and Engineering B, pp. 143-146 (1997).

Raman spectroscopy is used to study phonons in a series of thin (AlAs)m/(GaAs)n superlattices (SLs) grown by molecular beam epitaxy (MBE). The influence of buffer layer type and thickness on the interface roughness of heterostructures is carefully evaluated. The accuracy of optical phonons and the degree of peak sharpness of GaAs-like confined modes are examined via off-resonance Raman spectroscopy. Theoretical calculations of phonons in thin (AlAs)m/()GaAs)n superlattices (i.e., samples with m, n ^{2}12) are reported for various directions of propagation by using a rigid-ion model. Optical phonons acquire significant dispersive character when the wavevector **q** forming an angle **Θ** with the growth axis of the superlattice is changed from **Θ** = 0 to $\pi/2$ (i.e., from [001] to [100]). The frequency gaps in the angular dispersions due to mode anti-crossing behavior observed recently by Zunke et al. using micro-Raman spectroscopy are found to be in reasonably good agreement with our model calculations.
[Contact: Joseph G. Pellegrino, (301) 975-2123]

Analysis and Characterization Techniques

Released for Publication

Marchiando, J.F., Kopanski, J.J., and Lowney, J.R., **A Model Database for Determining Dopant Profiles from Scanning Capacitance Microscope Measurements**.

To help correlate scanning capacitance microscope measurements with dopant concentrations, model capacitance curves are calculated for uniformly doped silicon and stored in a database that depends on the probe-tip radius of curvature, the oxide thickness, and the dopant density. The oxide thicknesses range from 5 nm to 20 nm, the dopant concentrations range from 10^{17} cm^{-3} to 10^{20} cm^{-3}, and the probe-tip radius of curvature is set to 10 nm. The cone-shaped probe-tip is oriented normal to the sample surface, so that the finite-element method in two dimensions may be used to solve

Poisson's equation in the semiconductor region and Laplace's equation in the oxide and ambient regions. The equations are solved within the semi-classical quasi-static approximation, where the capacitance measurement depends only on the majority charge carriers, and inversion and charge trapping may be ignored. Comparison with one-dimensional-related models differs as much as 200% over the given doping range. For shallow gradient profiles satisfying quasi-uniformity conditions, the database is used directly to find the doping profile. Converting a 512 x 512 image takes less than 2 m. Comparison with a measured capacitance-voltage curve is briefly discussed.
[Contact: Jay F. Marchiando, (301) 975-2088]

Moreland, J., Russek, S.E., and Hopkins, P.F., **Surface Potential Imaging for MR Head Development**.

[See Magnetic Materials and Measurements.]

Analysis and Characterization Techniques

Recently Published

Kopanski, J.J., Marchiando, J.F., and Alvis, R., **Practical Metrology Aspects of Scanning Capacitance Microscopy for Silicon 2-D Dopant Profiling**, Extended Abstracts of the Electrochemical Society Spring 1997 Meeting, Montreal, Canada, May 4-9, 1997, p. 575.

A scanning capacitance microscope (SCM) acquires images of differential capacitance by either maintaining constant-voltage change, dV, or constant-capacitance change, dC, while simultaneously acquiring a topographic image with an atomic force microscope. When applied to prepared cross sections of silicon transistors, SCM images are acquired with contrast related to the two-dimensional (2-D) dopant distribution in the transistor. To convert SCM raw data to quantitative 2-D dopant profiles, the SCM's operating parameters must be selected to be in the regime that results in data that can be related simply to a model of the measurement. In this regime, SCM images can be converted to dopant profiles using a formalism that is both fast and accurate.
[Contact: Joseph J. Kopanski, (301) 975-2089]

Kopanski, J.J., Marchiando, J.F., Berning, D.W., Alvis, R., and Smith, H.E., **Scanning Capacitance Microscopy Measurement of 2-D Dopant Profiles Across Junctions**, Proceedings of the Fourth International Workshop on Measurement, Characterization and Modeling of Ultra-Shallow Doping Profiles in Semiconductors, Research Triangle Park, North Carolina, April 6-9, 1997, pp. 53.1–53.9.

Cross-sectioned p+/p and p-n junction test structures were imaged with a scanning capacitance microscope. To maintain a constant difference capacitance, our SCM utilizes an electronic attenuator circuit with a dynamic range of 20 V to less than 1 mV. Dopant profiles are extracted from SCM images using a formalism which rapidly determines the theoretical SCM response from a database of calculated C-V curves. A dopant profile from a p+/p junction determined via constant difference capacitance SCM is compared to a SIMS profile from similar structures.
[Contact: Joseph J. Kopanski, (301) 353-2089]

Krupka, J., Pietruszko, S., Geyer, R., Baker-Jarvis, J., and Derzakowski, K., **Semiconductor Resistivity Measurements Using Split Dielectric Resonator Technique**, Proceedings of the MIKON XI International Microwave Conference, Warsaw, Poland, May 27-30, 1996, Vol. 1, pp. 361-364.

[See Electromagnetic Properties.]

Device Physics and Modeling

Released for Publication

Adams, V.H., Joshi, Y., and Blackburn, D.L., **Three-Dimensional Study of Combined Conduction, Radiation, and Natural Convection from an Array of Discrete Heat Sources on a Horizontal Board in a Narrow-Aspect-Ratio Enclosure**.

[See Power Devices.]

Marchiando, J.F., Kopanski, J.J., and Lowney, J.R., **A Model Database for Determining Dopant Profiles from Scanning Capacitance Microscope Measurements**.

[See Analysis and Characterization Techniques.]

Device Physics and Modeling

Recently Published

Talwar, D.N., Roughani, B., Pellegrino, J.G., Amirtharaj, P.M., and Qadri, S.B., **Study of Phonons in Semiconductor Superlattices by Raman Scattering Spectroscopy and Microscopic Model Calculation**, Materials Science and Engineering B, pp. 143-146 (1997).

[See Compound Materials.]

Integrated-Circuit Test Structures

Recently Published

Lee, W.E., Guthrie, W.F., Cresswell, M.W., Allen, R.A., Sniegowski, J.J., and Linholm, L.W., **Reference-Length Shortening by Kelvin Voltage Tape in Linewidth Test Structures Replicated in Mono-Crystalline Silicon Films**, Proceedings of the 1997 IEEE International Conference on Microelectronic Test Structures, Monterey, California, March 18-20, 1997, pp. 35-38.

Electrical test structures replicated in thin films of single-crystal material offer potential benefits as physical standards for CD and overlay metrology. However, the regions where Kelvin voltage taps are attached typically have three-dimensional geometries. These geometries are uniquely predictable, except for a small measurable feature which is constant over large areas, and therefore offer an additional means for validating the linewidths of the bridge features. Current flow through these regions has been simulated, and the results have been compared with experimental measurements. A formulae has been calculated for the electrical length shortening effect of Kelvin-voltage taps, and this has been used to formulate a linewidth extraction algorithm.
[Contact: Michael W. Cresswell, (301) 975-2072]

Microfabrication Technology

Recently Published

Milanović, V., Gaitan, M., Bowen, E.D., Tea, N.H., and Zaghloul, M.E., **Design and Fabrication of Micromachined Passive Microwave Filtering Elements in CMOS Technology**, Proceedings of the 1997 International Conference on Solid-State Sensors and Actuators, Chicago, Illinois, June 16-19, 1997, pp. 1007-1010.

This paper describes a novel implementation of micromachined microwave resonators and filters, coupled with low-loss transmission lines, fabricated in standard CMOS technology. Selective etching of the Si substrate beneath the microwave elements results in significantly lowered transmission loss, improved quality factor, and operating frequency range. This allows operation at gigahertz frequencies. Resonators with Q-factors of 20 and resonant frequencies of 2 GHz and 21 GHz are reported which are significant results for standard CMOS technology. A low-pass filter is also reported with a 2.5 GHz cutoff frequency. The resonant and cutoff frequencies are, in general, adjustable within the 1 GHz to 40 GHz band. These devices are useful for integration with microwave power sensors, and have application in wireless communications systems where low-loss operation above 1 GHz is essential.
[Contact: Michael Gaitan, (301) 975-2070]

Milanović, V., Gaitan, M., Bowen, E.D., Tea, N.H., and Zaghloul, M.E., **Implementation of Thermoelectric Microwave Power Sensors in CMOS Technology**, Proceedings of the 1997 International Symposium on Circuits and Systems, Hong Kong, June 9-12, 1997, pp. 2753-2756.

[See Microwave and Millimeter-Wave Metrology.]

Milanović, V., Gaitan, M., Bowen, E.D., and Zaghloul, M.E., **Micromachined Microwave Transmission Lines in CMOS Technology**, IEEE Transactions on Microwave Theory and Techniques, Vol. 45, No. 5, pp. 630-635 (May 1997).

[See Microwave and Millimeter-Wave Metrology.]

Plasma Processing

Released for Publication

Rao, M.V.V.S., Olthoff, J.K., Christophorou, L.G.,

and Van Brunt, R.J., **Negative Ion Kinetic-Energy Distributions and Ion-Neutral Reactions in O_2 and CO_2 Townsend Discharges at High E/N**, to be published in the Proceedings of the 1997 International Symposium on Electron Molecule Collisions and Ion and Electron Swarms, Engelberg, Switzerland, July 18-22, 1997.

Electron attaching gases, such as O_2, CO_2, and SF_6, are commonly used ingredients in various gaseous discharges employed in plasma processing techniques. Negative ions formed in such gas discharges are known to influence the electrical discharge characteristics by altering the electron density. An understanding of the role played by negative ions in gas discharges and other applications requires a knowledge of their kinetics because negative ions can be converted to other charge carriers either by electron transfer or by electron detachment in collisions with neutrals. In this paper we report measurements of kinetic-energy distributions (KEDs) of O_2^- and O^- ions in O_2 and O^- in CO_2 discharges at high electric field-to-gas density ratios (*E/N*). The KEDs of the negative ions are explained by the possible electron-molecule collisions and ion-neutral reaction mechanisms. The mean ion energies are derived from the ion energy distributions and the relative abundance of the negative ions are determined from the flux measurements.
[Contact: James K. Olthoff, (301) 975-2431]

Rao, M.V.V.S., Van Brunt, R.J., and Olthoff, J.K., **Kinetic-Energy Distributions of Positive Ions Produced in Townsend Discharges of Oxygen at High Electric Field-to-Gas Density Ratios**, to be published in the Proceedings of the 1997 International Symposium on Electron Molecule Collisions and Ion and Electron Swarms, Engelberg, Switzerland, July 18-22, 1997.

Understanding the details of ion production and transport in electrical gas discharges is of importance to both the semiconductor industry, which uses gas-phase discharges for microelectronic device production, and the electric equipment industry, which uses electronegative gases as high-voltage insulation. Oxygen is a gas of interest in these areas because of its common usage in plasma discharges for etching and for cleaning processes, and also its nearly universal presence in high-voltage insulation systems as an impurity. In this report, we present measurements of kinetic-energy distributions (KEDs) for positive ions (O_2^+ and O^+) in oxygen, for dc Townsend discharges with electric field-to-gas density ratios (*E/N*) comparable to what may be found in the sheaths of radio-frequency plasmas. Analysis of these KEDs provided an insight into the production mechanisms of these ions, the dominant processes affecting the transport of the ions, and the validity of assuming equilibrium ion distributions at high values of *E/N*. From the measured KEDs, the mean ion energies are derived, and the relative ion intensities are obtained.
[Contact: Richard J. Van Brunt, (301) 975-2425]

Power Devices

Released for Publication

Adams, V.H., Joshi, Y., and Blackburn, D.L., **Three-Dimensional Study of Combined Conduction, Radiation, and Natural Convection from an Array of Discrete Heat Sources on a Horizontal Board in a Narrow-Aspect-Ratio Enclosure**.

Three-dimensional natural convection flow and heat transfer were numerically studied for a three-by-three array of discrete protruding heat sources on a horizontal substrate in an air-filled, rectangular, narrow-aspect-ratio enclosure with length, width, and height ratio of 6:6:1. The governing equations for natural convection in air, coupled with conjugate conduction and radiation within the enclosure, were solved using a finite volume method. The study examines the complex thermal interactions between the heat sources, substrate, and enclosure walls as affected by the thermal conductance of the walls and substrate. The influence of radiation on the overall heat transfer is given particular attention. The three-dimensionality of the problem was evident in the overall flow characteristics and in the convective heat transfer edge-effects on the heat surfaces. Excellent agreement between temperature predictions on the heat sources and substrate and experimental measurements was obtained for modified Rayleigh numbers in the range of 9.7×10^5 to 1.6×10^7.
[Contact: David L. Blackburn, (301) 975-2068]

Reliability

Released for Publication

Suehle, J.S., Chen, Y., and Bernstein, J., **A New Technique for Evaluating Reliability of Thin Gate Oxides**.

Results from time-dependent dielectric breakdown (TDDB) experiments indicate that electrically chargeable defects are not produced during low-electric field stress unlike that observed under high-electric field stress. Consequently, these quantities cannot be used as a measure of oxide damage accumulated during stress and correlated to oxide reliability. A Fowler-Nordheim injection technique used to evaluate process-induced damage has been applied to oxides subjected to constant field TDDB stress conditions. A latent damage was detected by changes in voltage versus time characteristics during a diagnostic constant current stress test and can be used as an indicator of oxide age independent of TDDB stress conditions.
[Contact: John S. Suehle, (301) 975-2247]

Reliability

Recently Published

Martin, A., O'Sullivan, P., Mathewson, A., Suehle, J.S., and Chaparala, P., **Investigation of the Influence of Ramped Voltage Stress on Intrinsic t_{bd} of MOS Gate Oxides**, Solid-State Electronics, Vol. 41, No. 7, pp. 1013-1020 (1997).

This study investigates the influence of a pre-stressing ramped voltage stress prior to a constant voltage stress on the time to breakdown. Constant voltage stress and combined ramped/constant voltage stress measurements were performed on six MOS gate oxide thicknesses. The time-to-breakdown distributions were compared, and an increase of the time to breakdown for pre-stressed oxides was observed in some cases. A further analysis of the current-time characteristics gave conclusions about the trapping properties of the oxide. It was found that the initial positive charge buildup in the oxide is an important indicator for degradation which must be considered for highly accelerated reliability measurements on pre-stressed oxides. Since common understanding of oxide breakdown and models for breakdown mechanisms cannot describe all of the experimental results, a qualitative model is proposed.
[Contact: John S. Suehle, (301) 975-2247]

SIGNAL ACQUISITION, PROCESSING, AND TRANSMISSION

DC and Low-Frequency Metrology

Released for Publication

Avramov-Zamurovic, S., Oldham, N.M., Parker, M., and Waltrip, B., **Low Frequency Characteristics of Thermal Voltage Converters**, to be published in the Proceedings of the 1997 IEEE Instrumentation and Measurement Technology Conference, Ottawa, Canada, May 19-21, 1997.

Low-frequency errors of multijunction thermal voltage converters are estimated using a simple model based on easily measured parameters. The model predictions are verified by measuring the converter's frequency characteristic using a digitally synthesized source.
[Contact: Nile M. Oldham, (301) 975-2408]

DC and Low-Frequency Metrology

Recently Published

Dulcie, L.L., **A Prototype Apparatus for Determining Changes in the Electrical Conductivity of Production Run Carbon Fibers**, Proceedings of the 22nd Annual Quantitative Non-Destructive Evaluation Conference, Seattle, Washington, July 31—August 4, 1995, pp. 2233-2239 (1997).

A prototype system was developed to detect the small changes in conductivity that occur in carbon fibers when either the heat treatment temperature (HTT) or resident furnace time varies during a production run. This system was designed using an optimized, encircling eddy current coil transducer, appropriate bridge electronics to detect and amplify the signal produced by coil impedance changes, and a voltage output proportional to changes in conductivity along the length of a carbon tow (multiple fibers). System measurement performance was evaluated by comparing the relative changes in output voltage between tows

with small variations in conductivities over the HTT range, 1600 °C to 2400 °C. The four-wire, dc apparatus developed earlier at NIST.
[Contact: Laura L. Dulcie, (303) 497-5606]

Croyelectronic Metrology

Released for Publication

Benz, S.P., Hamilton, C.A., Burroughs, C.J., and Christian, L.A., **Josephson Standards for AC Voltage Metrology**, to be published in the Proceedings of the 1997 National Conference of Standards Laboratories, Atlanta, Georgia, July 27-31, 1997.

[See FUNDAMENTAL ELECTRICAL MEASUREMENTS.]

Benz, S.P., Hamilton, C.A., Burroughs, C.J., Christian, L.A., and Przybysz, J.X., **A Pulse-Driven Josephson Digital/Analog Converter**, to be published in the Proceedings of the 1997 International Superconductive Electronics Conference, Berlin, Germany, June 25-28, 1997.

[See FUNDAMENTAL ELECTRICAL MEASUREMENTS.]

Benz, S.P., Hamilton, C.A., Burroughs, C.J., Harvey, T.E., and Christian, L.A., **Stable 1-Volt Programmable Voltage Standard**.

[See FUNDAMENTAL ELECTRICAL MEASUREMENTS.]

Li, H.Q., Ono, R.H., Vale, L.R., and Rudman, D.A., **High Temperature Superconducting Josephson Junctions in a Stacked Bicrystal Geometry**.

Bicrystal grain boundary Josephson junctions have been fabricated in a novel stack of two layers of $YBa_2Cu_3O_x$ separated by epitaxial $SrTiO_3$. Weak-link behavior was observed in bridges formed in both layers, with similar shunted-junction characteristics, but with significantly different critical currents. Characteristic voltages up to 1.9 mV were measured at 4.5 K. Resonant structure was seen in the current-voltage characteristics of the upper-layer junctions, and interactions between junctions in the two layers were evident.
[Contact: Ronald H. Ono, (303) 497-7705]

Ono, R.H., Li, H.Q., Vale, L.R., Rudman, D.A., and Liou, S.H., **Multilayer Processing of High-T_c Films and Josephson Devices**,

We present the results of a novel fabrication process that produces bicrystal junctions stacked one above the other. These high-temperature superconducting devices show conventional weak-link Josephson behavior and intriguing new phenomena, such as capacitively-coupled high-frequency interactions between junctions. Details of the fabrication process are shown.
[Contact: Ronald H. Ono, (303) 497-3762]

Reintsema, C.D., Koch, J.A., and Grossman, E.N., **A High Precision Electrical Substitution Radiometer Based on Superconducting-Resistive-Transition Edge Thermometry**.

We describe the design and measured performance of the first electrical substitution radiometer based on superconducting thermometers. The radiometer was originally conceived and developed for use in the Low Background Infrared Calibration Facility in Gaithersburg, Maryland. The application emphasizes high-precision measurement of low power, mid- and far-IR blackbody radiation. The minimum noise floor measured for the instrument was pW for an integration time of 2.7 s. For an extended series of experiments covering a range of substitution power from 0.5 nW to 5 μW, the noise floor can be roughly approximated as 4 pW plus 7 parts per million of the measured power. Analysis of the results indicates the precision is limited by a combination of thermal parasitics and electronic noise contributions.
[Contact: Carl D. Reintsema, (303) 497-5052]

Ruggiero, S.T., Rennert, K.J., Vale, L.R., and Rudman, D.A., **Properties of Co-Planar YBCO Devices**, to be published in the Proceedings of the 5th International Workshop on High-Temperature Superconductor Electron Devices, Matsuyama City, Japan, May 28-30, 1997.

We discuss work on co-planar YBCO thin-film devices. In these studies, systems are exposed to light from a mid-infrared (25 μm) diode laser monitored by a calibrated HgCdTe detector. For

the sample geometry studied here, we estimate an upper limit to the low-frequency responsivity, R, of ~1000 V/W. The co-planar systems themselves display a 5 GHz bandwidth and 50 Ω impedance for lines down to 2 μm in width.
[Contact: David A. Rudman, (303) 497-5081]

Cryoelectronic Metrology

Recently Published

Benz, S.P., and Burroughs, C.J., **Constant-Voltage Steps in Arrays of Nb-PdAu-Nb Josephson Junctions**, IEEE Transactions on Applied Superconductivity, Vol. 7, No. 2, pp. 2434-2437 (June 1997).

[See FUNDAMENTAL ELECTRICAL MEASUREMENTS.]

Benz, S.P., Burroughs, C.J., and Hamilton, C.A., **Operating Margins for a Pulse-Driven Programmable Voltage Standard**, IEEE Transactions on Applied Superconductivity, Vol. 7, No. 2, pp. 2653-2656 (June 1997).

[See FUNDAMENTAL ELECTRICAL MEASUREMENTS.]

Hamilton, C.A., Benz, S.P., Burroughs, C.J., and Harvey, T.E., **SNS Programmable Voltage Standard**, IEEE Transactions on Applied Superconductivity, Vol. 7, No. 2, pp. 2472-2475 (June 1997).

[See FUNDAMENTAL ELECTRICAL MEASUREMENTS.]

Hamilton, C.A., Burroughs, C.J., and Benz, S.P., **Josephson Voltage Standard - A Review**, IEEE Transactions on Applied Superconductivity, Vol. 7, No. 2, pp. 3756-3761 (June 1997).

[See FUNDAMENTAL ELECTRICAL MEASUREMENTS.]

Hamilton, C.A., Buroughs, C.J., Kupferman, S.L., Naujoks, G.A., and Vickery A., **A Compact Transportable Josephson Voltage Standard**, IEEE Transactions on Instrumentation and Measurement, Vol. 46, No. 2, pp. 237-241 (April 1997).

[See FUNDAMENTAL ELECTRICAL MEASUREMENTS.]

Huber, M.E., Cromar, M.W., and Ono, R.H., **Excess Low-Frequency Flux Noise in dc SQUIDs**, IEEE Transactions on Applied Superconductivity, Vol. 7, No. 2, pp. 2882-2885 (June 1997).

We have fabricated dc superconducting quantum interference devices (SQUIDS) incorporating Nb/Al-oxide/Nb Josephson junctions in both stripline and washer geometries. Low-frequency noise in excess of that predicted by the resistively-shunted junction model is present in both geometries and is demonstrated to the flux noise. This flux noise is not environmental. Improvements in fabrication processing over the past four years have reduced the level of this flux noise. SQUIDs are now fabricated with PdAu resistors, Nb wiring layers, and SiO_2 interlayer dielectric. In our best well-coupled SQUIDs, the white-noise energy sensitivity is 5×10^{-31} J·s, with a 1/f knee below 0.1 Hz. We believe further reduction in the flux noise might be obtained with the use of on-chip flux shielding and/or trapping structures.
[Contact: Ronald H. Ono, (303) 497-3762]

Kunkel, G., Hechtfischer, G., Frommberger, M., Veit, K., Kleiner, R., Muller, P., Prusseit, W., Kinder, H., Ferchland, L., Daalmans, G., and Ono, R.H., **Millimeter-Wave Radiation in High-T_c Josephson Junctions**, IEEE Transactions on Applied Superconductivity, Vol. 7, No. 2, pp. 3339-3342 (June 1997).

[See Microwave and Millimeter-Wave Metrology.]

Lee, A.T., Richard, P.L., Nam, S.W., Cabrera, B., and Irwin, K.D., **A Superconducting Bolometer with Strong Electrothermal Feedback**, Applied Physics Letters, Vol. 69, No. 12, pp. 1801-1803 (16 September 1996).

We present a theoretical analysis and experimental evaluation of a novel transition-edge superconducting bolometer for detecting infrared and millimeter waves. The superconducting film is voltage-biased, and the current is read by a

superconducting quantum interference device ammeter. Strong electrothermal feedback maintains the sensor temperature within the transition, gives a current responsivity that is simply the inverse of the bias voltage, suppresses Johnson and sensor 1/f noise, and reduces the response time by several orders of magnitude below the intrinsic time constant C/G. A voltage-biased bolometer was evaluated that operates on the $T_c \sim 95$ mK transition of a tungsten film with a thermal conductance of $G \sim 1.2 \times 10^{-9}$ W/K. As expected, the electrical noise equivalent power of 3.3×10^{-17} W/√Hz is close to the thermal fluctuation noise limit and is lower than that of other technologies for these values of G and temperature. The measured time constant of 10 μs is ~100 times faster than the intrinsic time constant.
[Contact: Kent D. Irwin, (303) 497-5911]

Li, H.Q., Ono, R.H., Vale, L.R., Rudman, D.A., Liou, S.H., and Mallison, W.H., **An Improved Multi-Layer Fabrication Process for $YBa_2Cu_3O_{7-x}$ Based Circuits**, IEEE Transactions on Applied Superconductivity, Vol. 7, No. 2, pp. 2169-2172 (June 1997).

Improved via connections in structures of $YBa_2Cu_3O_{7-x}/SrTiO_3/YBa_2Cu_3O_{7-x}$ (YBCO/STO/-YBCO) multilayers have been made using a combined HF wet-etching and ion-milling process. The critical current density J_c of the via is as high as 2×10^6 A/cm^2 at 76 K and is dominated by edge contacts to the ab-plane. YBCO and Sr_2AlNbO_6 (SAN) multilayer test circuits were also made with this process. The crossovers in a SAN test chip with 4° edge angles had a critical temperature T_c of 88 K and J_c of 1.5×10^6 A/cm^2 at 81 K, very close to those of the planar film, showing no evidence of weak links where the YBCO crosses low-angle SAN steps.
[Contact: Ronald H. Ono, (303) 497-3762]

Ono, R.H., Koch, J.A., Steinback, A., Huber, M.E., and Cromar, M.W., **Tightly Coupled dc SQUIDs with Resonance Damping**, IEEE Transactions on Applied Superconductivity, Vol. 7, No. 2, pp. 2538-2541 (June 1997).

We have reduced the effect of resonances on a washer style dc Superconducting Quantum Interference Device (SQUID) coupled to input flux transformers and analyzed our damping structures using a distributed circuit model. A resistance of 1 Ω is placed across each turn of a 137-turn coil coupled to a planar washer dc SQUID reducing the structure in the voltage-flux curve, thus extending the range of current biases over which the device operates. The energy sensitivity of the SQUID is predicted to not be degraded by the intra-coil resistors.
[Contact: Ronald H. Ono, (303) 497-3762]

Sanders, S.C., and Jeanneret, B., **Pt Buffer Layer for Protecting YBCO from Al at Annealing Temperatures up to 450°C**, Book Chapter in Advances in Cryogenic Engineering, L. T. Summers, Ed., Vol. 42 (Plenum Press, New York, New York, June 1997), pp. 877-882.

We have studied the effectiveness of different buffer layers to protect $YBa_2Cu_3O_{7-\delta}$ (YBCO) from aluminum when annealing at temperature up to 450 °C. Since Al is commonly used to form ohmic contacts to Si, these results have implications for potential hybrid superconductor-semiconductor applications. Buffer layers of Ag, Au, Au/Ag, Au/Cr, Au/Pt, and Pt were examined. The critical temperature T_c of the contact YBCO layer was measured before and after anneals at 300 °C to 450 °C in 1 atmosphere of O_2. Pt and Au/Pt were effective at preventing significant Al diffusion into YBCO and subsequent T_c degradation. The critical current density J_c could also be maintained when these buffer layers were employed.
[Contact: Steven C. Sanders, (303) 497-5096]

Vale, L.R., Ono, R.H., and Rudman, D.A., **$YBa_2Cu_3O_{7-\delta}$ Josephson Junctions on Bicrystal Al_2O_3 and $SrTiO_3$ Substrates**, IEEE Transactions on Applied Superconductivity, Vol. 7, No. 2, pp. 3193-3196 (June 1997).

Bicrystal grain-boundary junctions (bi-GBJs) have been reproducibly fabricated on $SrTiO_3$ (STO) and r-plane Al_2O_3 (sapphire) bicrystal substrates. Sapphire bicrystals are candidates for high-frequency applications due to their low dielectric constant and loss tangent. The sapphire bi-GBJs demonstrated resistively shunted junction (RSJ)-like current-voltage characteristics, with junction parameters comparable to the STO bi-GBJs and critical-current densities $J_c \sim 10^5$ A/cm^2.

Independent control of junction resistance (R_N) was demonstrated with the use of Au-shunt layers. In addition, overlayers such as Au or STO may act to passivate the GBJs and improve long-term stability. [Contact: Ronald H. Ono, (303) 497-3762]

Antenna Metrology

Released for Publication

Lieberman, A.G., and Vanderau, J.M., **Mobile Antennas**.

[See LAW-ENFORCEMENT STANDARDS.]

Muth, L.A., Wittmann, R.C., and Kent, B.M., **Measurement Assurance and Certification of Radar Cross Section Measurements**, to be published in the Proceedings of the 1997 National Conference of Standards Laboratories, Atlanta, Georgia, July 27-31, 1997.

A standard for radar cross section measurement assurance is being developed at the National Institute of Standards and Technology, and we discuss several aspects of its creation.

Uniform technical criteria are required to sustain and improve measurement quality. Determination of significant sources of errors, and the quantitative assessment of measurement uncertainty is fundamentally important. A fully developed measurement assurance program (MAP) goes beyond technical range characterization issues. Additional MAP features address range operations, interlaboratory comparisons, traceability, and documentation, to name a few.

To ensure that RCS ranges operate within standards established and accepted by the RCS community, periodic reviews of range MAPs are conducted by a certifying board composed of peers. Well-defined technical and managerial requirements must be satisfied for certification to be granted. NIST scientists will play a pivotal role in the certification process.
[Contact: Lorant A. Muth, (303) 497-3603]

Antenna Metrology

Recently Published

Masterson, K.D., Novotny, D.R., and Cavcey, K.H., **Standard Antennas Designed with Electrooptic Modulators and Optical-Fiber Linkage**, Proceedings of the SPIE (The International Society for Optical Engineering, P.O. Box 10, Bellingham, Washington 98227-0010), Intense Microwave Pulses IV, Vol. 2843, pp. 188-196 (August 1997).

[See Radiated EMI.]

Prickett, M.J., Bloomfield, R.A., Kinzel, G.A., Wittman, R.C., and Muth, L.A., **Uncertainty Analysis for NRaD Radar Cross Section Measurements**, NISTIR 5061 (April 1997).

The Naval Command, Control and Ocean Surveillance Center RDT&E Division conducts radar cross section measurements on U.S. naval ships and other targets. This document discusses the assessment of measurement uncertainty and follows general guidelines proposed by the National Institute of Standards and Technology.
[Contact: Ronald C. Wittman, (303) 497-3326]

Noise Metrology

Released for Publication

Kos, A.B., Russek, S.E., Kim, Y.K., and Cross, R.W., **Measurement of High Current Density Effects in GMR Spin Values for Magnetic Recording and Sensor Applications**.

[See Magnetic Materials and Measurements.]

Noise Metrology

Recently Published

McDonald, D.G., Phelan, R.J. Jr., Vale, L.R., Ono, R.H., Rice, J.P., Borcherdt, L., Rudman, D.A., Cosgrove, J., and Rosenthal, P., **Noise from YBCO Films: Size and Substrate Dependence**, IEEE Transactions on Applied Superconductivity, Vol. 7, No. 2, pp. 3091-3095 (June 1997).

Electrical noise measurements at 10 Hz are reported for YBCO films at the resistive edge. Results are given for films with widths of 0.1, 1, and 5 mm that were deposited simultaneously on the same substrate for three different substrate

materials. The noise equivalent temperature improves by approximately a factor of 10 as the thermometer area is increased by a factor of 2500, with fixed bias current. At temperatures giving maximum dR/dT and with nominally 19 mA bias currents, the 5 mm samples have very low noise equivalent temperatures of 3.1, 3.5, and 4.4 nK/√Hz for $LaAlO_3$, Al_2O_3, and Si substrates, respectively. These are the lowest values reported up to the present time. Surprisingly, noise from the sample on Si is consistent with pure Johnson noise even with bias current as large as 5 mA (0.28×10^4 A/cm^2). For YBCO thicknesses no greater than 50 nm, excellent thermometers can be made on any of these substrates in spite of the mechanical strains produced in the films by the substrate.
[Contact: Ronald H. Rice, (303) 497-3762]

Wait, D.F., and Randa, J., **Amplifier Noise Measurements at NIST**, IEEE Transactions on Instrumentation and Measurement, Vol. 46, No. 2, pp. 482-485 (April 1997).

We have recently measured the noise characteristics of two low-noise commercial amplifiers in the 2.0 GHz to 4.0 GHz frequency range. The tests were part of a program to develop and validate measurement methods for a noise-figure measurement service. Measured noise figures were about 0.5 dB ± 0.04 dB. We present the results and the accompanying uncertainties. We also describe the measurement method and summarize the many checks that were used to validate the method.
[Contact: David F. Wait, (303) 497-3610]

Microwave and Millimeter-Wave Metrology

Released for Publication

Booth, J.C., Beall, J.A., Ono, R.H., Stork, F.J.B., Rudman, D.A., and Vale, L.R., **Third-Order Harmonic Generation in High T_c Superconducting Coplanar Waveguides at Microwave Frequencies**, to be published in the Proceedings of the 1997 International Superconductive Electronic Conference, Berlin, Germany, June 25-28, 1997.

We use third harmonic measurements of coplanar waveguide (CPW) transmission lines to explore the behavior of nonlinearities in microwave devices fabricated from high T_c superconductors. Our measurements focus on the effect of varying the CPW geometry, including center linewidth and line length, on the nonlinearity of the circuit as measured by the third-order intercept. We find that the third-order intercepts decrease with increasing line length. We also find that differences in the third-order intercepts between lines of different linewidth can be explained quantitatively by the appropriate scaling of the incident microwave power. These observations show that the sources of nonlinearity in our CPW transmission lines are distributed in nature, and depend on the detailed form of the current distribution within the superconductor.
[Contact: James C. Booth, (303) 497-7900]

Juroshek, J., **A New Method for Measuring Source Mismatch of a Three-Port Coupler**.

A new method for measuring source mismatch of a three-port coupler is described. Measurements of source mismatch are required when a three-port coupler is used for power measurements or for calibrating other power sensors. The method, which is called the direct calibration method, uses conventional vector network analyzer one-port calibration techniques to determine the source mismatch of the coupler. Measurements are shown for both a 2 GHz to 18 GHz directional bridge and a 2 GHz to 50 GHz directional coupler. The accuracy of these measurements is very similar to the accuracy normally obtained for the measurements of source mismatch inside a vector network analyzer.
[Contact: John Juroshek, (303) 497-5362]

Williams, D.F., **Comments on "Simple Modeling of Coplanar Waveguide on Thick Dielectric over Lossy Substrate."**

A question is raised about the way in which the authors formulated the resistance of a coplanar waveguide over a lossy silicon substrate in the paper "Simple Modeling of Coplanar Waveguide on Thick Dielectric over Lossy Substrate."
[Contact: Dylan F. Williams, (303) 497-3138]

Microwave and Millimeter-Wave Metrology

Recently Published

Booth, J.C., Beall, J.A., DeGroot, D.C., Rudman, D.A., and Ono, R.H., **Microwave Characterization of Coplanar Waveguide Transmission Lines Fabricated by Ion Implantation Patterning of $YBa_2Cu_3O_{7-\delta}$**, IEEE Transactions on Applied Superconductivity, Vol. 7, No. 2, pp. 2780-2783 (June 1997).

We report on the application of Si and Al ion-implantation patterning to the fabrication of low-loss microwave transmission lines in high-temperature superconductor (HTS) thin films. Using this technique, we have fabricated coplanar waveguide transmission lines in $YBa_2Cu_3O_{7-\delta}$ thin films deposited on $LaAlO_3$ substrates. We have used both resonant and broadband measurements in order to characterize the performance of the resulting transmission line structures. For the broadband measurements, on-wafer calibrations were used to obtain accurate S-parameters and transmission line propagation constants up to 25 GHz. The propagation constants of the ion-implanted transmission lines do not differ significantly from those of lines patterned using conventional ion milling over the frequency range studied, with a value for the attenuation constant of approximately 0.03 dB/cm to 0.04 dB/cm at 5.0 K and 10 GHz. The relatively low losses of the ion-implanted devices demonstrate the effectiveness of this method of patterning for HTS microwave device fabrication.
[Contact: James C. Booth, (303) 497-7900]

Ginley, R.A., **Line-Reflect-Match Calibration Technique for the Dual Six-Port Automatic Network Analyzer**, IEEE Transactions on Instrumentation and Measurements, Vol. 46, No. 2, pp. 523-526 (April 1997).

A newly developed method allows dual six-port automatic network analyzers to be calibrated with a single, known one-port termination instead of air line standards. This technique is especially useful for calibrations below 30 MHz, where air lines cannot be adequately characterized. The choice of the value of the standard is also discussed.
[Contact: Ronald G. Ginley, (303) 497-3634]

Kunkel, G., Hechtfischer, G., Frommberger, M., Veit, K., Kleiner, R., Muller, P., Prusseit, W., Kinder, H., Ferchland, L., Daalmans, G., and Ono, R.H., **Millimeter-Wave Radiation in High-T_c Josephson Junctions**, IEEE Transactions on Applied Superconductivity, Vol. 7, No. 2, pp. 3339-3342 (June 1997).

We have investigated millimeter-wave radiation from single Josephson junctions and small phase-locked Josephson junction arrays. Josephson junctions were fabricated on sapphire bicrystal substrates. Emission could be measured up to 110 GHz. Resonances in ten-junction circuits yield linewidths narrower than 200 MHz. This type of array might be useful for applications in integrated receiver systems.
[Contact: Ronald H. Ono, (303) 497-3762]

Milanović, V., Gaitan, M., Bowen, E.D., Tea, N.H., and Zaghloul, M.E., **Design and Fabrication of Micromachined Passive Microwave Filtering Elements in CMOS Technology**, Proceedings of the 1997 International Conference on Solid-State Sensors and Actuators, Chicago, Illinois, June 16-19, 1997, pp. 1007-1010.

[See Microfabrication Technology.]

Milanović, V., Gaitan, M., Bowen, E.D., Tea, N.H., and Zaghloul, M.E., **Implementation of Thermoelectric Microwave Power Sensors in CMOS Technology**, Proceedings of the 1997 International Symposium on Circuits and Systems, Hong Kong, June 9-12, 1997, pp. 2753-2756.

This paper presents implementations of efficient microwave power measurement devices through commercial CMOS processes with additional maskless etching. Two types of detectors were fabricated and tested. Both types of thermocouple detectors measure true rms power of signals in the frequency range up to 20 GHz and input power range from -30 dBm to +10 dBm. The devices have linearity better than ±40% for output vs. input power over the 40 dB dynamic range. Measurements of the return loss, obtained using an automatic network analyzer, show an acceptable input return loss of less than -20 dB over the entire frequency range.
[Contact: Michael Gaitan, (301) 975-2070]

Milanović, V., Gaitan, M., Bowen, E.D., and Zaghloul, M.E., **Micromachined Microwave Transmission Lines in CMOS Technology**, IEEE Transactions on Microwave Theory and Techniques, Vol. 45, No. 5, pp. 630-635 (May 1997).

Coplanar waveguides were designed and fabricated through a commercial CMOS process with post-processing micromachining. The transmission-line layouts were designed with commercial computer-aided design tools. Integrated circuits were fabricated through MOSIS service, and subsequently suspended by top-side etching. The absence of the lossy silicon substrate after etching results in significantly improved insertion-loss characteristics, dispersion characteristics, and phase velocity. Two types of layout are presented for different ranges of characteristic impedance. Measurements of the waveguides, both before and after micromachining, were performed at frequencies from 1 GHz to 40 GHz using a vector network analyzer and de-embedding techniques, showing improvement of loss characteristics of orders of magnitude. For the entire range of frequencies, for the 50 Ω layout, losses do not exceed 4 dB/cm. These losses are mainly due to the small width and thickness of the metal strips. Before etching, losses are as high as 38 dB/cm due to currents in the underlying substrate. Phase velocity in the micromachined transmission lines is close to that in free space.
[Contact: Michael Gaitan, (301) 975-2070]

Walker, D.K., and Williams, D.F., **Compensation for Geometrical Variations in Coplanar Waveguide Probe-Tip Calibration**, IEEE Microwave and Guided Wave Letters, Vol. 7, No. 4, pp. 97-99 (April 1997).

We show how coplanar-waveguide probe-tip scattering parameter calibrations performed in one coplanar waveguide conductor geometry may be adjusted for measurement in another. The method models the difference between the two probe-tip-to-coplanar-waveguide transitions as a change in shunt capacitance, and applies previously developed techniques for its determination and compensation. Compensation to accurate multiline Thru-Reflect-Line calibrations verifies the accuracy of the method. Differences in both conductor geometry and substrate permittivity are considered in the comparison.
[Contact: David K. Walker, (303) 497-5490]

Williams, D.F., **Embedded Multiconductor Transmission Line Characterization**, Proceedings of the 1997 IEEE-MTT-S International Microwave Symposium Digest, Denver, Colorado, June 8-13, 1997, pp. 1773-1776.

This paper presents a measurement method that characterizes lossy printed multiconductor transmission lines embedded in transitions, connectors, or packages with significant electrical parasities. We test the method on a pair of lossy coupled asymmetric microstrip lines and compare to previous results.
[Contact: Dylan F. Williams, (303) 497-3138]

Electromagnetic Properties

Released for Publication

Geyer, R.G., and Vanderah, T.A., **Complex Permittivity and Permeability Estimation of Composite Electroceramics**, to be published in the Proceedings of the International Symposium on Dielectric Ceramics, American Ceramic Society International Meeting, Cincinnati, Ohio, May 4-7, 1997.

A modified form of Maxwell-Garnett effective medium theory is applied to the dielectric and magnetic characterization of two-phase media. Both the inclusions and host matrix of the composite ceramic may be magnetically permeable and possess dielectric and magnetic loss. The modified Maxwell-Garnett formulation does not yield symmetric characterization, and differs from other rules in that the loading particle permeability and permittivity properties are modified by a complex amplitude and phase-wave number function that quantifies how well electromagnetic fields penetrate the loading material. It may be used to give both upper and lower bounds for the effective permittivities and permeabilities of the composite and yield accurate estimates of bulk electric and magnetic properties for low-volumetric loading, once measurements are performed on the dielectric and magnetic properties of the individual constituent phases. A Bruggeman model for a two-phase

composite leads to a symmetric mixing rule, where effective dielectric and magnetic properties are evaluated from a complex quadratic involving the electric and magnetic properties of the individual constituents and the respective volume fractions. The Bruggeman model may be used for frequency-dependent dielectric property corrections of polycrystallites to theoretical density. Application to a ceramic $LaAlO_3$ sample having a density 20% less than theoretical yielded dielectric results that differed from single-crystal measured permittivities by no more than 4%.
[Contact: Richard G. Geyer, (303) 497-5852]

Paulter, N.G., **Long-Term Repeatability of a TDR-Based Printed Wiring Board Dielectric Constant Measurement Method**.

A new time-domain-reflectometry-based method has been recently developed that provides accurate determinations of the dielectric constant of printed wiring board dielectrics over the frequency range of 0.1 GHz to 10 GHz. The long-term measurement repeatability of that system was investigated, and the results are reported here.
[Contact: Nicholas G. Paulter, (301) 975-2405]

Weil, C.M., Baker-Jarvis, J.R., Geyer, R. G., Grosvenor, J.H., Janezic, M.D., Jones, C.A., Riddle, B.F., and Krupka, J., **Dielectric Characterization of Low-Loss Materials**.

Measurements on low-loss materials are presented using a number of measurement fixtures. Closed and open cavity resonators, surface-wave modes, and dielectric resonator methods were all used. Typical uncertainties associated with each method are addressed. Measurements were also performed on materials used in previous round robins.
[Contact: James R. Baker-Jarvis, (303) 497-5621]

Electromagnetic Properties

Recently Published

Geyer, R.G., and Krupka, J., **Microwave Behavior of Ferrites: Theory and Experiment**, Digest of the 1996 Conference on Precision Electromagnetic Measurements, Braunschweig, Germany, June 17-20, 1996, pp. 206-207.

The relative magnetic permeability and loss factor of microwave ferrites in the demagnetized state are determined near and above gyromagnetic resonance using low-loss dielectric ring resonators. This technique allows complex permeability determination on a single ferrite sample from 2 GHz to 25 GHz. The measured real parts of the initial permeability are compared with theoretical predictions of the permeability of a sample in the demagnetized state.
[Contact: Richard G. Geyer, (303) 497-5533]

Geyer, R.G., Krupka, J., Sengupta, L., and Sengupta, S., **Microwave Properties of Composite Ceramic Phase Shifter Materials**, Proceedings of the 1996 IEEE Conference of International Symposium for Applications of Ferroelectrics, New Brunswick, New Jersey, August 19-21, 1996, pp. 851-854.

The microwave properties of bulk ceramic barium strontium titanate and non-ferroelectric oxide composites are measured at X-band with a cylindrical mode-filtered resonant cavity. A helical wire-wound waveguide makes up the cavity's cylindrical wall, which permits the use of high-purity TE_{01n} resonant modes for high accuracy permittivity measurements. Measurement results at 300 K show that microwave dielectric losses increase as the stoichiometric percentage of barium increases. The real relative permittivity increases with decreasing weight percent of added non-ferroelectric low-loss oxide. Dielectric losses rapidly decrease with the addition of a relatively small amount of non-ferroelectric oxide.
[Contact: Richard G. Geyer, (303) 497-5852]

Krupka, J., Pietruszko, S., Geyer, R., Baker-Jarvis, J., and Derzakowski, K., **Semiconductor Resistivity Measurements Using Split Dielectric Resonator Technique**, Proceedings of the MIKON XI International Microwave Conference, Warsaw, Poland, May 27-30, 1996, Vol. 1, pp. 361-364.

A split dielectric resonator technique has been employed for resistivity measurements of semiconductors. Rigorous Rayleigh-Ritz and mode-matching methods are used for analysis. Bulk semiconductor wafers and thin amorphous silicon films deposited on fused silica substrates were

measured.
[Contact: Richard G. Geyer, (303) 497-5852]

Lewis, R.L., **Relative Permittivity Measurement of Rectangular Copper-Laminated Substrates Using the Full-Sheet Resonance Technique**, NISTIR 5062 (April 1997).

A measurement program has been undertaken at NIST to evaluate the full-sheet resonance (FSR) technique, from which consistent relative permittivity values have been obtained. We present an analysis of the theory underlying the FSR technique, along with a theoretical formulation correcting full two-port scattering-matrix measurements of a resonant cavity for the effects of coupling between the external measurement circuit and the cavity. A circuit analysis modeling the resonant cavity and its external circuit is presented, along with a least-squares solution for the resonant cavity's primary resonance parameters. The least-squares analysis features a slight rearrangement of an earlier formulation leading to a more numerically stable solution. An even earlier solution for a resonant cavity's unloaded quality factor, also using a least-squares solution to obtain a coupling correction, is presented for comparison. The application of these coupling correction formulations to the FSR technique is discussed, and results from these two correction formulations are compared with uncorrected results for two sample FSR panels. Computed least-squares data-scatter uncertainties are obtained for each FSR permittivity measurement, which are then used to obtain overall uncertainty estimates for each panel's measured permittivity, including a repeatability uncertainty estimate. These overall uncertainty estimates are compared to our earlier uncorrected FSR uncertainty estimate, showing a tightening of the uncertainty interval for corrected measurements. Finally, our measured FSR permittivities are compared with re-entrant cavity substrate permittivity measurements, showing agreement within expected uncertainty limits between the two techniques.
[Contact: Richard L. Lewis, (303) 497-5916]

Stork, F.J.B., Beall, J.A., Roshko, A., DeGroot, D.C., Rudman, D.A., Ono, R.H., and Krupka, J., **Surface Resistance and Morphology of YBCO Films as a Function of Thickness**, IEEE Transactions on Applied Superconductivity, Vol. 7, No. 2, pp. 1921-1924 (June 1997).

[See Electromagnetic Properties.]

Complex System Testing

Released for Publication

Hans, E., Souders, M., and Stenbakken, G.N., **Efficient Testing of Electronic Devices**, to be published in the Proceedings of the Interface 97 Conference, Houston, Texas, May 14-17, 1997.

Testing electronic devices in order to assure the quality of individual products can be time-consuming and expensive. To speed up this process without compromising on reliability, testing strategies have been developed at NIST. They are based on the extraction of low-dimensional linear error models, using a prior knowledge of the structure of the device or data from an exhaustively tested training and validation set. Production testing then is performed only on a small subset of all possible test points which must be chosen carefully. This paper describes statistical and computational aspects of these procedures and reports on the theoretical background, heuristics, algorithms, and practical experiences.
[Contact: T. Michael Souders, (301) 975-2406]

ELECTRICAL SYSTEMS

Power Systems Metrology

Released for Publication

Martzloff, F.D., **Considerations on Electromagnetic Immunity of Single-Phase Personnel Protection Devices**, to be published as NISTIR 6023.

A review is given of U.S. and international standards concerning electromagnetic immunity requirements for Personnel Protection devices, with suggestions for appropriate levels in order to prevent electric shock hazards and spurious trip-out of electric vehicle battery chargers.
[Contact: François D. Martzloff, (301) 975-2409]

Martzloff, F.D., **Power Quality Work at the**

International Electrotechnical Commission, to be published in the Proceedings of the 1997 Power Quality Applications Europe Conference, Stockholm, Sweden, June 16-19, 1997.

This paper presents an update, including a brief historical background on the work to be undertaken at the International Electrotechnical Commission to address power issues. To be useful, this work must take into consideration the three principal stakeholders, namely the producers of electric power, the manufacturers of equipment that use electric power, and the users of that equipment. Other stakeholders include manufacturers of power quality monitors, manufacturers of line conditioners, and power quality consultants. At this time, there are some differences of perceptions on how the work can be accomplished to best serve the interests of all stakeholders. Nevertheless, there is no disagreement on the first goal to be reached, which is to catalyze development of compatible, comparable, and consistent results in the measurement of power quality parameters.
[Contact: François F. Martzloff, (301) 975-2409]

Wang, Y., **New Method for Measuring Statistical Distributions of Partial Discharge**, to be published in the Journal of Research of the National Institute of Standards and Technology.

A new digital detection system is described for measuring pulsating partial discharges (PDs). The PD-detection system can continuously record all PD pulses that occur over extended periods of time, with a minimum inter-pulse time resolution of 6 μs and a vertical amplitude resolution of 12 bits. The present system differs from previously reported digital PD detection systems mainly in that the early systems detect PD-pulse amplitude and time with custom-designed hardware, while the present system continuously records the complete electrical waveform that carries the PD pulses with a commercial data acquisition board and extracts, in real time, the time and amplitude information of all PD pulses in software. The current approach considerably reduces the development and maintenance cost of a PD-detection system, significantly increases the system portability, and may prove to be a crucial step for transferring the digital PD detection and analysis technology developed in laboratories to industry. The new system is demonstrated by employing it to study dc-excited PD pulses occurring in a point-to-plane gap in air. A new surface-enhanced burst mode of PD is discovered in which a PD pulse has a certain probability to induce another pulse. The probability is determined for several gap voltages and is found to vary strongly with the applied voltage.
[Contact: James K. Olthoff, (301) 975-2431]

Wang, Y., Han, X., Van Brunt, R.J., Horwath, J., and Schweichart, D., **Digital Recording and Analysis of Positive Partial Discharges in Air**, to be published in the Proceedings of the 12th International Conference on Gas Discharges and Their Applications, Greifswald, Germany, September 8-12, 1997.

A new surface-mediated burst mode of partial discharges is discovered in which a partial discharge pulse has a fixed probability to induce a following pulse, forming a burst of evenly-separated pulses. The probability is determined for several gap voltages and is found to vary strongly with the applied voltage.
[Contact: Richard J. Van Brunt, (301) 975-2425]

Magnetic Materials and Measurements

Released for Publication

Brooks, R.A., Vymazal, J., Goldfarb, R.B., Bulte, J.W., and Aisen, P., **Iron Uptake and Core Formation in Ferritin: Relaxometry and Magnetometry Studies**.

A unique combination of magnetometry and nuclear magnetic relaxometry studies on 44 ferritin samples, with iron loadings from 0 to 3400 atoms per molecule, has yielded the following results. The ferritin core is shown to be antiferromagnetic at least to 37 °C, with antiferromagnetic formation beginning after about 10 Fe atoms are bound per molecule. In addition, a superparamagnetic (SPM) moment is present in 1/3 to 1/6 of the cores, due to incomplete cancellation of antiferromagnetic sublattices. The SPM moment decreases with increasing temperature, and is responsible for T2 relaxations (which has an anomalous linear dependence on field strength). Besides these "uncancelled" Fe atoms, there is an additional iron fraction (up to 11%) that is paramagnetic and

causes T1-shortening.
[Contact: Ronald B. Goldfarb, (303) 497-3650]

Kirschenbaum, L.S., Rogers, C.T., Russek, S.E., and Kim, Y.K., **Low-Frequency Noise in NiFe/Cu Spin-Valves**.

We report one of the first observations of low-frequency noise of NiFe/Cu spin-valves. Although the observed noise is very low in comparison to multilayer systems, it is typically concentrated in the linear response region where such devices are expected to operate. Increased noise is also associated with Barkhausen jumps in the magnetoresistance trace. In 1 μm height devices, structures in the noise spectra start to appear as a perturbation to the simple 1/f-like noise observed in larger devices.
[Contact: Stephen E. Russek, (303) 497-5097]

Kos, A.B., Russek, S.E., Kim, Y.K., and Cross, R.W., **Measurement of High Current Density Effects in GMR Spin Values for Magnetic Recording and Sensor Applications**.

High-current density measurements on giant magnetoresistive (GMR) NiFe-Cu-NiFe-FeMn spin-valve devices are presented. The spin-valve response is highly temperature dependent; at temperatures near the blocking temperature, there is a considerable reduction of pinning field and decrease in device response. It is desirable to measure certain high-current density effects such as electromigration and self-field effects separately from thermal effects. In this paper, we present pulsed current techniques as a method to reduce thermal effects from wafer-level device measurements.
[Contact: Stephen E. Russek, (303) 497-5097]

Moreland, J., Russek, S.E., and Hopkins, P.F., **Surface Potential Imaging for MR Head Development**.

We present the first application of scanning surface potential microscopy to magnetoresistive (MR) thin-film devices. Surface potential microscopy based on atomic force microscopy currently offers 50 nm lateral spatial and 1 mV to 10 mV voltage sensitivity. We present data on active devices showing 2D maps of the surface potential of energized MR read-head stripes at puck level in the production line. We also show that surface potential line scans along MR spin-valve stripes show deviations from linearity possible due to nonuniform film magnetization along the length of the stripe.
[Contact: John Moreland, (303) 497-3641]

Magnetic Materials and Measurements

Recently Published

Cross, R.W., and Kos, A.B., **Relaxation in NiFe/Ag Giant Magnetoresistive Devices**, Journal of Applied Physics, Vol. 79, No. 8, pp. 5820-5822, (April 1996).

Giant magnetoresistance was measured as a function of time and device size for patterned NiFe/Ag multilayer films. The sputtered NiFe/Ag multilayers were post-annealed at 340 °C for 5 min, in order to produce a change in resistivity $\Delta\rho/\rho$ of 5% in a saturating field of 4 kA/m (50 Oe). The microstructure of these films is believed to be discontinuous due to Ag bridging through the NiFe grain boundaries after the anneal. The films were fabricated into rectangular stripes with Au-current leads, and then exposed to a magnetic-field pulse in order to measure the time response of the resistance, characterized by a time constant τ from the relation $\Delta R(t) = \Delta R_0 e^{-t/\tau}$. An apparatus was developed to produce a magnetic-field pulse up to 8 kA/m (100 Oe) with a turn on/off time constant of 10 μs. The response of the NiFe/Ag devices saturated quickly with the turn-on pulse up with a time constant nearly equal to that of the field pulse. The response to the turn-off pulse, however, had a time constant of nearly 300 μs. When the field is first applied, the torque on the magnetic moments quickly aligns the magnetization. When the field is shut off, however, the torque due to the field drops to zero, so that interacting magnetostatic fields from the grains and thermal energy dominate the relaxation process. The time constant was found to depend on the device size and the applied current density. For devices smaller than a micrometer, steps and jumps were observed in the relaxation response due to individual grains (or clusters) switching. Relaxation effects may be very detrimental for using this material for read heads where high data rates are required.
[Contact: Ralph W. Cross, (303) 497-5300]

Hopkins, P.F., Thomson, R.E., Moreland, J., Malhotra, S.S., and Liou, S.H., **Magnetic Force Microscopy Using Fe-(SiO_2) Coated Tips**, Digest of the 1995 IEEE International Magnetics Conference, San Antonio, Texas, April 18-21, 1995, p. CS-05.

[See Analysis and Characterization Techniques.]

Hu, X., **Magnetization Reversal and Coercive Force in Ultrathin Films With Perpendicular Surface Anisotropy: Micromagnetic Theory**, Physical Review B, Vol. 55, No. 13, pp. 55 8382–55 8389 (1 April 1997).

Quasi-static magnetization reversal in ultrathin magnetic films with perpendicular surface anisotropy is discussed. In order to focus on the role of the surface anisotropy, magnetization is presumed uniform across the film plane, and its variation along the film normal is subject to micromagnetic analysis of a functional including the shape anisotropy energy from dipolar interactions. Different reversal processes—such as nucleations, coherent and incoherent rotations, domain-wall motion, and abrupt jumps—are found in films, depending on the values of shape anisotropy, surface anisotropy, exchange stiffness, and film thickness. The coercivity of ultrathin magnetic films in fields perpendicular to the film plane decreases with the square of the reciprocal of the film thickness, which coincides very well with experimental observations. Magnetization reversal processes resulting from applying in-plane external fields are also described. [Contact: Xiao Hu, (303) 497-3701]

Shafi, K.V.P.M., Gedanken, A., Goldfarb, R.B., and Felner, I., **Sonochemical Preparation of Nanosized Amorphous Fe-Ni Alloys**, Journal of Applied Physics, Vol. 81, No. 10, pp. 6901-6905 (May 1997).

Nanosized amorphous alloy powders of $Fe_{20}Ni_{80}$, $Fe_{40}Ni_{60}$, and $Fe_{60}Ni_{40}$ were prepared by sonochemical decomposition of solutions of volatile organic precursors, $Fe(CO)_5$ and $Ni(CO)_4$ in decalin, under an argon pressure of 100 kPa to 150 kPa at 273 K. Magnetic susceptibility of $Fe_{40}Ni_{60}$ and $Fe_{60}Ni_{40}$ indicates blocking temperatures of 35 K and a magnetic particle size of about 6 nm. Thermogravimetric measurements of $Fe_{20}Ni_{80}$ give Curie temperatures of 322 °C for amorphous and 550 °C for crystallized forms. Differential scanning calorimetry exhibits an endothermic transition at 335 °C from a combination of the magnetic phase transition and alloy crystallization. The Mossbauer spectrum of crystallized $Fe_{20}Ni_{80}$ shows a sextet pattern with a hyperfine field of 25.04 T. [Contact: Ronald C. Goldfarb, (303) 497-3650]

Superconductors

Released for Publication

Booth, J.C., Beall, J.A., Ono, R.H., Stork, F.J.B., Rudman, D.A., and Vale, L.R., **Third-Order Harmonic Generation in High T_c Superconducting Coplanar Waveguides at Microwave Frequencies**, to be published in the Proceedings of the 1997 International Superconductive Electronic Conference, Berlin, Germany, June 25-28, 1997.

[See Microwave and Millimeter-Wave Metrology.]

Li, H.Q., Ono, R.H., Vale, L.R., and Rudman, D.A., **High Temperature Superconducting Josephson Junctions in a Stacked Bicrystal Geometry**.

[See Cryoelectronic Metrology.]

Ruggiero, S.T., Rennert, K.J., Vale, L.R., and Rudman, D.A., **Properties of Co-Planar YBCO Devices**, to be published in the Proceedings of the 5th International Workshop on High-Temperature Superconductor Electron Devices, Matsuyama City, Japan, May 28-30, 1997.

[See Cryoelectronic Metrology.]

Superconductors

Recently Published

Booth, J.C., Beall, J.A., DeGroot, D.C., Rudman, D.A., and Ono, R.H., **Microwave Characterization of Coplanar Waveguide Transmission Lines Fabricated by Ion Implantation Patterning of $YBa_2Cu_3O_{7-\delta}$**, IEEE Transactions on Applied Superconductivity, Vol. 7, No. 2, pp. 2780-2783 (June 1997).

[See Microwave and Millimeter-Wave Metrology.]

Bray, S.L., Ekin, J.W., and Sesselmann, R., **Tensile Measurements of the Modulus of Elasticity of Nb_3Sn at Room Temperature and 4 K**, IEEE Transactions on Applied Superconductivity, Vol. 7, No. 2, pp. 1451-1454 (June 1997).

The critical current of Nb_3Sn superconductors is highly sensitive to strain. Consequently, accurate mechanical modeling of these conductors is necessary to interpret experimental data and to predict conductor performance in applications such as large magnet systems. A key parameter in these models is the modulus of elasticity (E. Young's modulus); however, there are large discrepancies in the available data, and there are no published tensile-test data on E for Nb_3Sn. Tensile test specimens were prepared from a starting material of Nb tape with 1.4 wt% ZrO_2 precipitates. Tensile measurements of unreacted Nb and partially reacted Nb-Nb_3Sn tapes were made at room temperature (293 K) and at 4 K. A modulus of elasticity of 65 ± 15 GPa was extrapolated from these measurements for polycrystalline Nb_3Sn at 4 K, and 150 ± 15 GPa at room temperature.
[Contact: Steven L. Bray, (303) 497-5631]

Cooley, L.D., Lee, P.J., and Larbalestier, D.C., **Flux-Pinning Mechanism of Proximity-Coupled Planar Defects in Conventional Superconductors: Evidence That Magnetic Pinning is the Dominant Pinning Mechanism in Niobium-Titanium Alloy**, Physical Review B, Vol. 53, No. 10, pp. 6638-6652 (March 1996).

The bulk flux-pinning force curve $F_p(H)$ of optimized Nb-Ti superconducting wires, made conventionally or by artificial pinning-center (APC) design, changes in magnitude and shape at constant temperature T and exhibits a lack of temperature scaling at constant wire diameter. We propose that this behavior occurs because magnetic pinning is the dominant mechanism over core pinning for the ribbon-shaped, proximity-coupled pins. Because the magnetic pinning force $f_p(H)$ then is nonmonotonic when the pin thickness t is near the proximity length ϵ_N, the lack of temperature scaling and the change in magnitude and shape of $F_p(H)$ at constant T are direct consequences of the pinning mechanism. The optimum $F_p(H)$ curve occurs when a balance between strong f_p and a high-number density of pins is reached, usually when $t \sim \epsilon_N/3$ and often not when t equals the diameter of the fluxon core. Pins made from clean metals and alloys, such as Nb, lack high-field pinning because ϵ_N is too long. We find verification of our predictions in $F_p(H,T,t)$ data for special laboratory-scale APC wires, for which extensive microstructural characterization by TEM was obtained.
[Contact: Lance D. Cooley, (303) 497-7747]

Ekin, J.W., **Electromechanical Properties of Bi-2212 Superconductors**, Proceedings of the 9th U.S.-Japan Workshop on High-Field Superconducting Materials, for High-Field Superconducting Wire Testing, Kyoto, Japan, March 13-15, 1997, pp. 143-148.

The axial strain degradation of the critical current of $Bi_2/Sr_2/Ca_1Cu_2O_{8+x}$ (Bi-2212) round-wire superconductors has been measured for Ag- and AgNiMg-sheathed wires. A direct comparison between Ag- and AgNiMg-sheathed Bi-2212 conductors having the same number of filaments, matrix superconductor ratio, and overall wire diameter shows that the irreversible strain limit for the AgNiMg-sheathed conductors is significantly higher than for the Ag-sheathed conductors. The higher yield strength of AgNiMg compared with Ag may explain both the increased strain tolerance and lower degradation rate in the AgNiMg-sheathed wires. We observe that, for both types of sheathing materials, Bi-2212 round-wire conductors with filament diameters down to about 0.1 mm have the highest J_c values and the lowest strain limit to irreversible J_c damage.
[Contact: John W. Ekin, (303) 497-5448]

Ekin, J.W., and Bray, S.L., **High Compressive Axial Strain Effect on Critical Current and Field of Nb_3Sn Superconductor Wire**, Advances in Cryogenic Engineering, Vol. 42, pp. 1407-1414 (June 1997).

The axial strain dependence of the critical current I_c and upper critical field B_{c2}^* has been measured on a series of Nb_3Sn superconductors having initial compressive strain as large as -0.95% arising from thermal contraction of the conductor matrix. Results include data for binary Nb_3Sn wire and ternary Nb_3Sn wire with Ti additions. The I_c and B_{c2}^* data

are fit well by the strain scaling law; they are consistent with earlier published T_c data for Nb_3Sn at compressive strain as large as -0.85%, and with I_c data for stainless-steel reinforced Nb_3Sn superconductors at compressive strain as large as -0.65%. The data contradict, however, recently reported B_{c2}^* data obtained on multifilamentary Nb_3Sn wires where high compressive strain was applied by soldering the wires to a bending beam.
[Contact: John W. Ekin, (303) 497-5448]

Ekin, J.W., Bray, S.L., Joshi, C.H., and Rodenbush, A.J., **Effect of Strain on the Critical Current of High-T_c Bi Superconductors and an Epoxy-Impregnated Bi Superconducting Coil**, Critical Currents in Superconductors, Harald W. Weber, Ed., World Scientific, pp. 659-662 (June 1997).

The effect of axial strain (applied at 4 K) on the critical current I_c of several Ag-sheathed Bi superconductors has been measured and compared with the effect of hoop strain (also applied at 4 K) on the I_c of a 50-turn coil of Bi superconductor wrapped with fiberglass and potted with epoxy. The data suggest that the I_c strain limit on the composite coil structure is imposed not by the Bi superconductor, but by the fracture properties of the epoxy used to impregnate the coil. Thus, magnet coil degradation is not an intrinsic limit imposed by the mechanical fracture limits of present Bi superconductors, but appears to be amenable to improvement through choice of epoxy and coil structure design.
[Contact: John W. Ekin, (303) 497-5448]

Goodrich, L.F., Medina, L.T., and Stauffer, T.C., **Repeatability of Critical-Current Measurements on Nb_3Sn and NB-Ti Wires**, IEEE Transactions on Applied Superconductivity, Vol. 7, No. 2, pp. 1508-1511 (June 1997).

A varying degree of repeatability has been observed in critical-current (I_c) measurements of Nb_3Sn and Nb-Ti wires as a function of the number of thermal cycles from room temperature to 4 K. The increase of I_c between the first and second thermal cycle can be 1% to 2% at 12 T for Nb_3Sn wires. This was observed on a Nb_3Sn wire by all four laboratories that participated in a recent interlaboratory comparison conducted in the International Thermonuclear Experimental Reactor (ITER) project. These data indicate that if I_c changes beyond the error limits, it increases fairly monotonically with thermal cycling until it eventually saturates. In contrast, the I_c of a Nb-Ti wire is very repeatable with thermal cycling. This suggests that the effect on the Nb_3Sn wire is due to its strain sensitivity. Most of these data were taken with the sample on a Ti-6Al-1V measurement mandrel. This study also investigated the repeatability of I_c measurements using other mandrel materials. The increase in I_c of Nb_3Sn wire could enhance the performance of some applications. However, the lack of repeatability in I_c measurements on Nb_3Sn wires is a limitation in precise interlaboratory comparisons.
[Contact: Loren F. Goodrich, (303) 497-3143]

Gregory, E., Gulko, E., Pyon, T., and Goodrich, L.F., **Improvements in the Properties of Internal-Tin Nb_3Sn Strands**, Proceedings of the 16th International Cryogenic Engineering Conference/International Cryogenic Materials Conference, Kitakyushu, Japan, May 20-24, 1996, pp. 1715-1718 (1997).

In papers given a year ago, the results of round-robin testing of International Thermonuclear Experimental Reactor (ITER) type Nb_3Sn conductors have shown the variation of their J_c's with field. The EGC conductor, as heat treated to meet the ITER specification at 12 T, showed a steeper curve of J_c against field than that of the other designs, suggesting a lower H_{c2} and T_c. Since the temperature and time of the heat treatment were restricted in order to ensure that the residual resistivity ratio was not reduced by chromium diffusion, the slope of the curve had to be changed by means other than a simple heat treatment change. In this paper, a series of conductors with increased H_{c2} and T_c and significantly reduced ac losses, are described.
[Contact: Loren F. Goodrich, (303) 497-3143]

Gregory, E., Gulko, E., Pyon, T., and Goodrich, L.F., **Properties of Internal-TIN Nb_3Sn Strand for the International Thermonuclear Experimental Reactor**, Advances in Cryogenic Engineering, Vol. 42, pp. 1319-1328 (July 1996).

We report on the design and properties of a Nb_3Sn wire strand developed for the International

Thermonuclear Experimental Reactor (ITER). The internal-tin process was employed using 19 subelements, six spacers, and a Ta-containing barrier to separate the superconducting core from the Cu stabilizer. Specific values of the four properties - critical current density J_c, hysteresis losses, residual resistivity ratio RRR, and piece length - required by the ITER specification are difficult to achieve simultaneously in one strand design. This is particularly true when the strand is Cr plated to prevent sintering and to provide interstrand resistance. Some aspects of conductor design and heat treatment, and how these affect the various properties, including *n* value, are outlined.
[Contact: Loren F. Goodrich, (303) 497-3143]

McDonald, D.G., Phelan, R.J., Jr., Vale, L.R., Ono, R.H., Rice, J.P., Borcherdt, L., Rudman, D.A., Cosgrove, J., and Rosenthal, P., **Noise from YBCO Films: Size and Substrate Dependence**, IEEE Transactions on Applied Superconductivity, Vol. 7, No. 2, pp. 3091-3095 (June 1997).

[See Noise Metrology.]

Stork, F.J.B., Beall, J.A., Roshko, A., DeGroot, D.C., Rudman, D.A., Ono, R.H., and Krupka, J., **Surface Resistance and Morphology of YBCO Films as a Function of Thickness**, IEEE Transactions on Applied Superconductivity, Vol. 7, No. 2, pp. 1921-1924 (June 1997).

We have examined the thickness dependence of the growth morphology and surface resistance R_s of laser-ablated $YBa_2Cu_3O_{7-\delta}$ films with transition temperatures over 89 K and critical current temperatures over 89 K and critical current densities greater than 10^6 A/cm^2 at 76 K. The thickness was varied from 50 nm to 1600 nm, while all other deposition conditions were maintained constant. The microstructure has been characterized by scanning electron microscopy and scanning tunneling microscopy. The films exhibit two-dimensional island growth at all thicknesses, and the island density continuously decreased with film thickness as a power law with an exponent of -0.5. The surface resistance was measured at 76 K with a dielectric rod resonator. For films less than 300 nm thick, the fields penetrated the superconducting films, causing a rapid increase in the apparent R_s with decreasing film thickness. Films thicker than 800 nm showed microcracks and R_s increased sharply, and no resonance was observed above 1000 nm.
[Contact: Donald C. DeGroot, (303) 497-7212]

Xu, Y., Ekin, J.W., Russek, S.E., Fiske, R., and Clickner, C.C., **a-Axis $YBa_2Cu_3O_{7-\delta}$/Au Interface Conductance-Voltage Characteristics**, IEEE Transactions on Applied Superconductivity, Vol. 7, No. 2, pp. 2836-2839 (June 1997).

Conductance-voltage characteristics of interfaces between n-axis $YBa_2Cu_3O_{7-\delta}$ (YBCO) thin films and gold are presented. When the gold counter electrode is deposited *in-situ*, the junctions have a specific interface resistivity in the 10^{-9} Ω-cm^2 range, about an order of magnitude lower than nominal *in-situ*, c-axis YBCO/noble-metal junctions. As with nominal c-axis YBCO/noble-metal junctions, there is clear evidence at T = 4 K for a peak in the conductance at low bias. In addition, a dip in the middle of the broad-peak structure was resolved. It appears to be a feature unique to the a-axis YBCO/Au interface.
[Contact: Stephen R. Russek, (303) 497-5097]

ELECTROMAGNETIC INTERFERENCE

Radiated EMI

Recently Published

Hill, D.A., and Kanda, M., **Measurement Uncertainty of Radiated Emissions**, NIST Technical Note 1389 (March 1997).

We present a summary of current knowledge and techniques for evaluating measurement uncertainty of radiated emissions. The important quantity for compliance testing is the expanded uncertainty (typically for a coverage factor k = 2), and we discuss the validity of obtaining the combined uncertainty from an RSS sum of separate uncertainties. A generic uncertainty model includes the following separate sources of measurement uncertainty: setup of equipment under test, measurement procedure, facility, antenna, and receiver. Measurement uncertainties for radiated emissions are large and not well quantified, and recommendations are made for further study.
[Contact: David A. Hill, (303) 497-3472]

Holloway, C.L., DeLyser, R.R., German, R.F., McKenna, P., and Kanda, M., **Comparison of Electromagnetic Absorber Used in Anechoic and Semi-Anechoic Chambers for Emissions and Immunity Testing of Digital Devices**, IEEE Transactions on Electromagnetic Compatibility, Vol. 39, No. 1, pp. 33-47 (February 1997).

The absorber used in anechoic and semi-anechoic chambers employed for emissions and immunity testing of digital devices is examined. Using reflectivities obtained by the method of homogenization, the advantages and disadvantages of urethane pyramids, twisted-pyramids, and wedges, as well as ferrite tiles, ferrite grids, and "hybrid" combinations of urethanes and ferrites, are determined. General reflectivity guidelines are also presented for comparing absorber used for the electromagnetic compatibility testing of digital devices from 30 MHz to 1000 MHz.
[Contact: Motohisa Kanda, (303) 497-5320]

Masterson, K.D., Novotny, D.R., and Cavcey, K.H., **Standard Antennas Designed with Electrooptic Modulators and Optical-Fiber Linkage**, Proceedings of the SPIE (The International Society for Optical Engineering, P.O. Box 10, Bellingham, Washington 98227-0010), Intense Microwave Pulses IV, Vol. 2843, pp. 188-196 (August 1997).

We described the design of standard reference antennas that utilizes an electro-optic transducer together with optical-fiber linkage to preserve the amplitude and phase information of the received signal. They will be used over a range from 10 MHz to 2 GHz at our open area test site in order to reduce measurement uncertainties attributable to the ambient electromagnetic spectrum. The transducer consists of an optical-fiber directional coupler with unbalanced legs and $LiNbO_3$ phase environments. The complementary rf signal is modeled to determine the design and operating parameters required for good repeatability and accuracy. The results show that spurious reflections in the modulator legs need to be less than -50 dB in order to obtain the desired stability.
[Contact: Keith D. Masterson, (303) 497-3756]

Masterson, K.D., Novotny, D.R., and Koepke, G.H., **The Electromagnetic Shielding Characteristics of Optical-Fiber Connectors**, NIST Technical Note 1383 (April 1997).

A number of commercially available fiber optic connector styles (ST, SC, and FC) were tested to determine the extent to which their use in bulkhead adapter feedthroughs would compromise the shielding of electromagnetic interference for electronic enclosures. Metal, ceramic, and polymer components were included in the test matrix. Tests were carried out using a nested reverberation cell technique and cover a frequency range from 1 GHz to 16 GHz. The shielding effectiveness varied widely, from a low of about 20 dB to a high for an all-metal FC connector system that was nearly equal to the 90 dB obtained for a blank reference plate. In some cases, the feedthrough coupled more energy into the enclosure than was coupled through the empty hole required to mount the adapter barrel. Comparison between the experimental results and the theory for coupling electromagnetic energy through a circular aperture enables us to more accurately determine the *Q* of the nested cell and to calculate transmission cross sections for the feedthroughs. The calculated transmission cross sections are not dependent on the specific experimental parameters and can be used to estimate the degradation in shielding effectiveness for enclosures other than our reference cell. The inaccuracies in the reported transmission cross sections are calculated to be ± 3 dB and are small compared to the differences between the measured cross sections.
[Contact: Keith D. Masterson, (303) 497-3756]

LAW-ENFORCEMENT STANDARDS

Released for Publication

Lieberman, A.G., and Vanderau, J.M., **Mobile Antennas**.

NIJ Standard 0205.02, Mobile Antennas, establishes minimum structural, environmental, and radio frequency performance requirements and test methods for antennas that are mounted on police vehicles or other mobile platforms used by law enforcement agencies. Antenna performance is addressed for the following law enforcement frequency bands: 25 MHz to 50 MHz, 150 MHz to 174 MHz, 406 MHz to 512 MHz, and 806 MHZ to 930 MHz.

[Contact: A. George Lieberman, (301) 975-2757]

OPTOELECTRONICS

Released for Publication

Bertness, K.A., Hickernell, R.K., and Christensen, D.H., **Wobble Normalization for Optical In Situ Measurements in Molecular Beam Epitaxy**, to be published in the Proceedings of the 16th North American Conference on Molecular Beam Epitaxy, Ann Arbor, Michigan, October 5-8, 1997.

Analysis of in-situ optical measurements taken during molecular beam epitaxy is usually hindered by large periodic variations in collection efficiency as the sample wobbles slightly about its rotation axis. We describe a technique for removing the periodic wobble effect by correlating the optical in-situ signal with a signal from an angular position sensor on the substrate rotation mechanism. Only those data points at particular trigger positions are kept, and these are normalized by an average curve taken at times when no change in the optical signal is expected. We find that this process reduces the wobble effect by at least a factor of ten in both normal incidence optical reflectance and in reflection-mode atomic absorption measurements. Key factors in making this technique work have been (1) careful budgeting of computer time during data acquistion, (2) use of several triggers per rotation to allow accurate normalization even for rotation speed variations on the order of $\pm$15%, and (3) use of a 0th trigger to recover from accidental loss of trigger synchronization.
[Contact: Kristine A. Bertness, (303) 497-3319]

Franzen, D.L., Mechels, S.E., and Schlager, J.G., **Differential Mode Delay Measurements in Multimode Fibers Using a Frequency Domain Technique with Variable Launch**, to be published in the Conference Digest on Optical Fiber Measurements, Teddington, United Kingdom, September 29—October 1, 1997.

Differential mode delay (DMD) profiles are determined for multimode fibers using a frequency domain phase shift technique. A time resolution of 0.2 ps is achieved, making measurements on short lengths of fiber possible; comparisons with more traditional time domain methods on longer lengths show agreement. DMD profiles obtained on several 62 μm diameter core fibers exhibit a diverse range of behavior.
[Contact: Douglas L. Franzen, (303) 497-3346]

Lehman, J.H., **Pyroelectric Trap Detector for Spectral Responsivity Measurements**.

We have designed and built a pyroelectric optical detector for use as a transfer standard for the calibration of optical power meters. The pyroelectric element is made from $LiTaO_3$, and gold black is used as the optical absorber in a multiple reflection wedge-shaped trap structure which has a 5 mm diameter input aperture and an f/4 field of view. The detector spatial responsivity varies less than 1%. The responsivity as a function of wavelength varies less than 1% over a range from 0.45 μm to 10.6 μm. The measured noise equivalent power is 5×10^{-8} W/Hz$^{1/2}$. For this wavelength range and detector area, the measured NEP and spatial uniformity represent a significant improvement over comparable predecessors.
[Contact: John H. Lehman, (303) 497-3654]

Mechels, S.E., Franzen, D.L., and Wicks, M., **International Comparison: Final Report**.

This report presents the results of an international comparison of optical fiber dispersion measurements between NIST and the National Physical Laboratory (UK). Both labs used frequency-domain phase shift systems to measure the optical wavelength at which chromatic dispersion in a single-mode fiber goes to zero. This wavelength is an important parameter in high bandwidth telecommunication systems. The results of the two laboratories agreed to within the uncertainties of the systems.
[Contact: Stephen E. Mechels, (303) 497-5409]

Obarski, G.E., and Jones, R.D., **Polarization States Behave as Hyperfine Levels in VCSEL Mode Partition Noise**.

We show how correlations between relative intensity noise (RIN) and beam profile geometry of a vertical-cavity surface-emitting laser, in a single transverse LP_{11} mode, demonstrate mode partition noise based on spatial overlap of orthogonal polarization components and polarization degeneracies. For a

wide range of drive current, the RIN of each polarization component is at least 20 dB/Hz greater than that of the total beam, with a greatest difference of 40 dB/Hz to 45 dB/Hz.
[Contact: Gregory E. Obarski, (303) 497-5747]

Rochford, K.B., and Rose, A.H., **Linear Retardance Standard Reference Material**, to be published in the Proceedings of the SPIE (The International Society for Optical Engineering, P.O. Box 10, Bellingham, Washington 98227-0010), Optical Science, Engineering, and Instrumentation, San Diego, California, July 27—August 1, 1997.

Polarimetric systems often require linear retarders with well-characterized performance. NIST has developed a Standard Reference Material that can be used to calibrate polarimetric instruments and improve measurement accuracy. The device provides nominally 90° retardance at 1219 nm, with the actual value known to within ±0.1°. The design and performance of this device is reviewed and the procedure for certification outlined.
[Contact: Kenneth B. Rochford, (303) 497-5170]

Rose, A.H., and Rochford, K.B., **Packaging Hygroscopic and Stress-Sensitive Optics for a Standard Retarder**, to be published in the Proceedings of the SPIE (The International Society for Optical Engineering, P.O. Box 10, Bellingham, Washington 98227-0010), Optical Science, Engineering, and Instrumentation, San Diego, California, July 27—August 1, 1997.

We discuss the optomechanical design and construction of a standard retarder. The retarder is a double Fresnel rhomb device. With our device, we have achieved retardance stability within ±0.1 °C over a ±20 °C temperature range and an estimated 10 year lifetime for storage within normal laboratory temperature and humidity conditions. The retardance of an optical rhomb retarder is sensitive to stress-induced birefringence. We selected a glass with a low-stress optic coefficient to improve optical performance. However, the glass is hygroscopic, and the retardance of the device changes in the presence of water vapor. Thus, for a stable retardance, a package as hermetic to water as possible that does not introduce any stress birefringence is required. We have tested the permeability of the seals and the sensitivity of our optical device to water vapor, and predicted a usable lifetime for the retarder. We discuss the optical materials, water permeability of seal materials, and the mathematical models used to predict the lifetime of the device. Also, we discuss the optical design and retarder's placement in the package to minimize stress-induced birefringence.
[Contact: Allen H. Rose, (303) 497-5599]

Schlager, J.B., Mechels, S.E., and Franzen, D.L., **High Resolution Differential Mode Delay and Bandwidth Measurements in Multimode Fibers**, to be published in the Proceedings of the 1997 IEEE Lasers and Electro-Optics Society Annual Meeting, San Francisco, California, November 10-13, 1997.

Differential mode delay measurements in multimode fibers are performed using a frequency domain phase shift technique capable of 0.2 ps temporal resolution. Measurements give insight into the behavior of fiber bandwidth with respect to launching conditions.
[Contact: John B. Schlager, (303) 497-3542]

Vander Rhodes, G.H., Pomeroy, J.M., Ulu, G., Ünlü, M.S., Goldberg, B.B., Knopp, K.J., and Christensen, D.H., **Direct Measurement of Pump Field Distributions in an Optically Pumped Vertical-Cavity Surface-Emitting Laser**, to be published in the Proceedings of the 1997 IEEE Lasers and Electro-Optics Society Annual Meeting, San Francisco, California, November 10-13, 1997.

Near-field scanning optical spectroscopy is used to map the pump field in an optically pumped vertical-cavity surface-emitting laser. The local spontaneous emission measurement along the cleaved edge parallel axis correlates to the pump profile.
[Contact: David H. Christensen, (303) 497-3354]

Veasey, D.L., Gary, J.M., and Amin, J., **Time Dependent Modeling of 980-nm Pumped Erbium-Doped Waveguide Lasers in Lithium Niobate**.

We have developed a rigorous theoretical model for analyzing rare-earth-doped waveguide laser devices. The model is based on the time-dependent laser rate equations for an arbitrary

multilevel rare-earth-doped laser host. These rate equations are coupled with the laser signal and pump propagating wave equations with time-dependent boundary conditions. The formulation results in a large and stiff set of transcendental-coupled differential equations which are solved using finite difference discretization and the method of lines. Solutions for the laser signal power, pump power, and populations of ion energy levels as functions of space and time, are obtained for waveguide lasers. We have used the model to predict the continuous wave characteristics and Q-switch performance of 980 nm end-pumped erbium-doped waveguide lasers fabricated in lithium niobate. Moreover, we have compared the cw and Q-switch performance of 980 nm pumped waveguide lasers and 1480 nm pumped waveguide lasers. An analysis of the effect of host and fabrication dependent parameters on continuous wave 980 nm pumped lasers is included. These parameters include cooperative up-conversion, excited state absorption, doping concentration, excess waveguide loss, cavity length, and reflectance values. We show good quantitative agreement with actual waveguide laser experimental data obtained in our laboratory and with results presented in other literature.
[Contact: David L. Veasey, (303) 497-5192]

OPTOELECTRONICS

Recently Published

Amin, J., Aust, J.A., and Sanford, N.A., **Z-Propagating Waveguide Lasers in Rare-Earth-Doped Ti:$LiNbO_3$**, Applied Physics Letters, Vol. 69, No. 25, pp. 3785-3787 (December 1996).

A means of reproducibly fabricating stable cw lasers in rare-earth-doped Ti:$LiNbO_3$ has been demonstrated through judicious choice of waveguide orientation. Z-propagating waveguides have been fabricated in Nd- and Er-diffused Ti:$LiNbO_3$ and room-temperature laser operation with greatly reduced photorefractive instability has been obtained. The reduced photorefractive damage susceptibility in this waveguide configuration has led to the realization of a 980 nm pumped laser in Er:$TiLiNbO_3$, with a threshold of 10.5 mW of absorbed pump power and a slope efficiency of 8.5%.
[Contact: J. Andrew Aust, (303) 497-3942]

Amin, J., Aust, J.A., Veasey, D.L., and Sanford, N.A., **980 nm-Pumped Er- and Er/Yb-Doped Waveguide Lasers in $LiNbO_3$**, Proceedings of the 1997 European Conference on Integrated Optics, Stockholm, Sweden, April 2-4, 1997, pp. PD8-1—PD8-4.

We demonstrate a 980 nm pumped Er- and the first Er/Yb-doped waveguide laser in Ti:$LiNbO_3$. The devices were fabricated on x-cut $LiNbO_3$, with the guides parallel to the z-axis. This choice of waveguide orientation results in a reduced susceptibility to photorefractive damage and allows cw room-temperature operation.
[Contact: J. Andrew Aust, (303) 497-3942]

Aust, J.A., Steiner, B., Sanford, N.A., Fogarty, G., Yang, B., Roshko, A., Amin, J., and Evans, C., **Examination of Domain-Reversed Layers in Z-Cut LiNbO Using Maker Fringe Analysis, Atomic Force Microscopy, and High-Resolution X-Ray Diffraction Imaging**, Proceedings of the 1997 Conference on Lasers and Electro-Optics, Baltimore, Maryland, May 18-23, 1997, pp. 485-486.

Domain-inverted regions on z-cut LiNbO plates were examined using Maker fringe analysis, atomic force microscopy, high-resolution X-ray topography, and optical interferometry. Domain-inverted layers native to the +z faces of the samples were examined in addition to electric-field-poled sections.
[Contact: Andrew J. Aust, (303) 497-3942]

Christensen, D.H., Hill, J.R., Hickernell, R.K., Matney, K., and Goorsky, M.S., **Evaluating Epitaxial Growth Stability**, Materials Science and Engineering B, pp. 113-116 (1997).

We have investigated variations of epitaxial layer thickness from uniform periodicity in compound semiconductor Bragg-reflectors experimentally and theoretically. Specifically, we characterized the variation of individual layer thicknesses in the growth direction at a given point on the wafer, thereby assessing the growth stability in time. The characterization is based on the correlation of experimental reflectance spectroscopy and high-resolution X-ray diffractometry measurements and

precisely fitted simulations made on growth runs which include random and systematic variations from perfect periodicity. We find good agreement between the measurement techniques and between the measurements and their simulations.
[Contact: David H. Christensen, (303) 497-3354]

Masterson, K.D., Novotny, D.R., and Cavcey, K.H., **Standard Antennas Designed with Electrooptic Modulators and Optical-Fiber Linkage**, Proceedings of the SPIE (The International Society for Optical Engineering, P.O. Box 10, Bellingham, Washington 98227-0010), Intense Microwave Pulses IV, Vol. 2843, pp. 188-196 (August 1997).

[See Radiated EMI.]

Masterson, K.D., Novotny, D.R., and Koepke, G.H., **The Electromagnetic Shielding Characteristics of Optical-Fiber Connectors**, NIST Technical Note 1383 (April 1997).

[See Radiated EMI.]

Obarski, G.E., and Jones, R.D., **Relative Intensity Noise Correlates with Beam Profile in an LP_{11} Mode Vertical-Cavity Surface-Emitting Laser**, Proceedings of the 1997 Conference on Lasers and Electro-Optics, Baltimore, Maryland, May 18-23, 1997, pp. 228-229.

We show how correlations between relative intensity noise and beam profile geometry of a vertical-cavity surface-emitting laser, in single-transverse LP_{11} mode, support a mode partition of the noise based on spatial overlap of orthogonal polarization components and polarization degeneracies.
[Contact: Richard D. Jones, (303) 497-3439]

Rochford, K.B., Rose, A.H., and Wang, C.M., **NIST Study Investigates Retardance Uncertainty**, Laser Focus World, Vol. 33, No. 5, pp. 223-227 (May 1997).

NIST recently performed an intercomparison of retardance measurements to sample current practice and found adequate measurement accuracy for the majority of current applications, but possibly inadequate accuracy for the most critical retarder needs.
[Contact: Kenneth B. Rochford, (303) 497-5170]

Rose, A.H., **Devitrification in Annealed Optical Fiber**, Journal of Lightwave Technology, Vol. 15, No. 5, pp. 808-814 (May 1997).

The decrease in transmittance of annealed optical fiber has been measured vs. temperature and time. The annealing loss is due to the devitrification of the glass and OH absorption in the 1200 nm to 1500 nm wavelength region. Both loss mechanisms propagate primarily from the surface into the core. However, to increase the OH absorption significantly, annealing times greater than 10 h are required. Fibers heated from 1000 °C to 1300 °C have been measured. A decrease in the current sensitivity is attributed to devitrification in the fiber.
[Contact: Allen H. Rose, (303) 497-5599]

Rose, A.H., Etzel, S.M., and Wang, C.M., **Verdet Constant Dispersion in Annealed Optical Fiber Current Sensors**, Journal of Lightwave Technology, Vol. 15, No. 5, pp. 803-807 (May 1997).

The Verdet constant in annealed optical fiber current sensors has been measured at wavelengths from 636 nm to 1320 nm. The measurements are fitted to two models, one classical and the other an expansion of the classical model that includes a nonlinear term. These measurements and models are compared to previous measurements made in optical fiber and bulk SiO_2. Our measurements have an average accuracy of $\pm 0.6\%$ and an average measurement of $\pm 0.5\%$ over the 636 nm to 1320 nm range.
[Contact: Alan H. Rose, (303) 497-5599]

VIDEO TECHNOLOGY

Released for Publication

Fenimore, C.P., Field, B.F., and Van Degrift, **Test Patterns and Quality Metrics for Digital Video Compression**, to be published in the Proceedings of the SPIE (The International Society for Optical Engineering, P.O. Box 10, Bellingham, Washington 98227-0010), Symposium on Electronic Imaging 97 Human Vision and Electronic Imaging II, San Jose, California, February 10-13, 1997.

Lossy video compression systems such as MPEG2 introduce picture impairments such as image

blocking, color distortion, and persistent color fragments, "mosquito noise," and blurring in their outputs. While there are video test clips which exhibit one or more of these distortions upon coding, there is need of a set of well-characterized test patterns and video quality metrics. Digital test patterns can deliver calibrated stresses to specific features of the encoder, much as the test patterns for analog video stress critical characteristics of that system. Metrics quantify the error effects of compression by a computation.
[Contact: Charles P. Fenimore, (301) 975-2428]

X-RAY SPECTROMETRY

Released for Publication

Hilton, G.C., Martinis, J.M., Twerenbold, D., Gillevet, P.M., Wollman, D.A., Irwin, K.D., Dulcie, L.L., and Gerber, D., **Energy-Resolving Cryogenic Particle Detectors for Time-of-Flight Mass Spectrometry**.

Time-of-flight spectrometry techniques, most notably matrix-assisted laser-desorption-ionization time-of-flight spectrometry, have become increasingly important in the study of proteins and other biomolecules. While these techniques provide excellent performance for masses up to about 20 KDa, there has been limited success in achieving good mass resolution at higher masses. It has been proposed that cryogenic particle detectors might provide a solution to these difficulties. Recent experiments have demonstrated the sensitivity of cryogenic particle detectors to single biomolecules, and a quantum efficiency several orders of magnitude larger than the microchannel plate detectors used in conventional spectrometers. Here, we present results demonstrating the use of energy-resolving cryogenic particle detectors for mass spectrometry. By measuring the thermal energy deposited by a particle impact, we can determine the charge state of the particle during acceleration. These detectors also provide new insight into the collision process and may prove useful in optimizing future time-of-flight spectrometers.
[Contact: Gene C. Hilton, (303) 497-5679]

Martinis, J.M., Wollman, D., Irwin, K., and Hilton, G.C., **Microcalorimeter X-Ray Spectrometers**.

A revolutionary advance in X-ray microanalysis will occur in the next few years due to the development of new X-ray spectrometers based on microcalorimeters. These detectors will be similar in operation to commonly-used energy dispersive spectrometers, but will improve upon the energy resolution by at least a factor of 10, thus rivaling or possibly exceeding the resolution achievable with wavelength dispersive spectrometers. We discuss the basic operating principle of this new technology and present microanalysis data taken with the detector on a scanning electron microscope to demonstrate the utility of the microcalorimeter spectrometer. Its primary impact on semiconductor process metrology will be improved analysis of low energy (100 eV to 2 keV) X-rays. This capability is important for detection of light elements, resolving interferences in important materials such as WSi_2 and TiN, and defect review.
[Contact: John M. Martinis, (303) 497-3597]

Martinis, J.M., Wollman, D.A., Irwin, K.D., and Hilton, G.C., **Superconducting Microcalorimeter X-Ray Spectrometers**, to be published in the Proceedings of the 1997 International Superconductive Electronics Conference, Berlin, Germany, June 25-28, 1997.

A revolutionary advance in X-ray microanalysis will occur in the next few years due to the development of new X-ray spectrometers based on microcalorimeters. These detectors will be similar in operation to commonly-used energy dispersive spectrometers, but will improve upon the energy resolution by at least a factor of 10, thus rivaling or possibly exceeding the resolution achievable with wavelength dispersive spectrometers. We discuss the basic operating principle of this new technology and present microanalysis data taken with the detector on a scanning electron microscope to demonstrate the utility of the microcalorimeter spectrometer.
[Contact: John M. Martinis, (303) 497-3597]

Wollman, D.A., Irwin, K.D., Hilton, G.C., Dulcie, L.L., Newbury, D.E., and Martinis, J.M., **High-Energy-Resolution Microcalorimeter Spectrometer for X-Ray Microanalysis**.

We are developing a high-energy-resolution X-ray microcalorimeter spectrometer for use in X-ray

microanalysis. The microcalorimeter spectrometer system consists of a superconducting transition-edge sensor X-ray microcalorimeter cooled to an operating temperature near 100 mK by a compact adiabatic demagnetization refrigerator, a Superconducting Quantum Interference Device current amplifier followed by pulse-shaping amplifiers and pileup reject circuitry, and a multichannel analyzer with computer interface for the real-time acquisition, we have achieved an instrument response energy resolution of better than 10 eV full width at half maximum (FMHM) over a broad energy range at real-time output count rates to 150 counts per second. Careful analysis of digitized X-ray pulses yields a microcalorimeter instrument response energy resolution of 7.2 eV + 0.4 eV FWHM at 5.89 keV for Mn Kα1, 2 X-rays from a radioactive ^{55}Fe source, the best reported energy resolution for any energy-dispersive detector.
[Contact: David A. Wollman, (303) 497-7457]

X-RAY SPECTROMETRY

Recently Published

Lee, A.T., Richard, P.L., Nam, S.W., Cabrera, B., and Irwin, K.D., **A Superconducting Bolometer with Strong Electrothermal Feedback**, Applied Physics Letters, Vol. 69, No. 12, pp. 1801-1803 (16 September 1996).

[See Cryoelectronic Metrology.]

ADDITIONAL INFORMATION

Announcements

Knight, S., and Settle-Raskin, A., **Project Portfolio FY 1997 - The National Semiconductor Metrology Program**, NISTIR 5851 (May 1997).

The National Semiconductor Metrology Program (NSMP) is a NIST-wide effort designed to meet the highest priority measurement needs of the semiconductor industry as expressed by the *National Technology Roadmap for Semiconductors* and other authoritative industry sources. The NSMP was established in 1994 with a strong focus on mainstream silicon CMOS technology and an ultimate funding goal of $25 million annually. Current annual funding of approximately $11 million supports the 24 internal projects which are summarized in the Project Portfolio booklet.

The NSMP is operated by NIST's Office of Microelectronics Programs, which also manages NIST's relationships with the Semiconductor Industry Association (SIA), SEMATECH, and the Semiconductor Research Corporation (SRC). These include NIST's memberships on the SIA committees that develop the *Roadmap* and numerous SRC technical management committees. In addition, NIST is active in the semiconductor standards development activities of American Society for Testing and Materials (ASTM), Deutsches Institut für Normung (DIN), Electronic Industries Association (EIA), International Organization for Standardization (ISO), and Semiconductor Equipment and Materials International (SEMI).
[Contact: Steven Knight, (301) 975-2871]

Lists of Publications

Bradford, A.G., **Metrology for Electromagnetic Technology: A Bibliography of NIST Publications**, NISTIR 5051 (September 1996).

This bibliography lists the publications of the personnel of the Electromagnetic Technology Division of NIST during the period from January 1970 through publication of this report. A few earlier references that are directly related to the present work of the Division are also included. This edition of the bibliography is the first since the Electromagnetic Technology Division split into two Divisions, and it includes publications from the areas of cryoelectronic metrology and superconductor and magnetic measurements. The optical electronic metrology section found in earlier editions is now being produced separately by the new Optoelectronics Division of NIST. That companion bibliography to this publication is NISTIR 5052.
[Contact: Ann G. Bradford, (303) 497-3678]

Lyons, R.M., **A Bibliography of the NIST Electromagnetic Fields Division Publications**, NISTIR 5050 (August 1996).

This bibliography lists the publications by the staff of the National Institute of Standards and Technolo-

gy's Electromagnetic Fields Division for the period January 1970 through July 1996. It supersedes NISTIR 5039 which listed the publications of the Electromagnetic Fields Division from January 1970 through July 1995. Selected earlier publications from the Division's predecessor organizations are included.
[Contact: Ruth Marie Lyons, (303) 497-3132]

Schmeit, R.A., **Electrical and Electronic Metrology: A Bibliography of NIST Electricity Division's Publications, NIST List of Publication 94** (March 1997).

This bibliography covers publications of the Electricity Division (and predecessor organizational units), Electronics and Electrical Engineering Laboratory, National Institute of Standards and Technology, for the period of January 1968 through December 1996. A brief description of the Division's technical program is given in the introduction.
[Contact: Ruth A. Schmeit, (301) 975-2401]

Smith, A.J., **A Bibliography of Publications of the NIST Optoelectronics Division**, NISTIR 5052 (September 1996).

This bibliography lists publications of the staff of the Optoelectronics Division and its predecessor organizational units from 1970 through the date of this report.
[Contact: Annie J. Smith, (303) 497-5342]

Walters, E.J., **NIST List of Publications 103, National Semiconductor Metrology Program and the Semiconductor Electronics Division, 1990-1996** (March 1997).

This List of Publications includes all papers relevant to semiconductor technology published by NIST staff, including work of the National Semiconductor Metrology Program and the Semiconductor Electronics Division, and other parts of NIST having independent interests in semiconductor metrology. Bibliographic information is provided for publications from 1990 through 1996. Indices by topic area and by author are provided. Earlier reports of work performed by the Semiconductor Electronics Division (and its predecessor divisions) during the period from 1962 through December 1989 are provided in NIST List of Publications 72.
[Contact: E. Jane Walters, (301) 975-2050]

1997-1998 Calendar of Events

October 16, 1997 (Austin, Texas)

Ion Implant Users Group Meeting. The meeting is in conjunction with SEMICON South West 95. The meeting provides a forum for the informal exchange of information and ideas of ion-implant-related issues, their future trends and applications. This year's meeting, "Opportunities and Challenges in Ion Implantation," is organized by the Ion Implant Users Group (East Coast), the Greater Silicon Valley Implant Users Group, and the Greater Southwest Implant/RTP Users Group. The topics for this meeting include Nitrogen Implants for Defect Engineering, High-Dose Hydrogen Implants for SOI Applications, the Use of Indium and Antimony as Alternatives to Boron, Phosphorus for Shallow-Junction Formation, Trends in Ultra-Low Energy Implantation, and High-Energy Implantation.
[Contact: John Albers, (301) 975-2075]

October 30-31, 1997 (Gaithersburg, Maryland)

Workshop on Thin Dielectric Films. The Semiconductor Electronics Division of NIST is conducting a two-day workshop on thin dielectric film metrology. This workshop includes invited speakers and discussion groups focused on issues pertinent to the setup and calibration for optical metrology tools (primarily ellipsometers and reflectometers), the use of standards, traceability of standards to NIST, and ways to address related evolving industry requirements for thin dielectric films. This workshop will be particularly beneficial for manufacturers of such optical metrology tools, those in integrated circuit manufacturers' calibration laboratories, and those involved with NIST-traceable or secondary thin dielectric film standards. The workshop concludes with a round-table discussion of closely related issues such as metrology for developing thin-gate dielectrics, the relationship between optical, electrical, and other film characterization techniques, and what the projected necessary standards are for developing technologies.
[Contact: Barbara J. Belzer, (301) 975-2248]

November 4-7, 1997 (Shanghai, China)

International Conference on Materials and Process Characterization for VLSI, 1997 (ICMPC'97). Co-sponsored by NIST and Institute of Microelectronics in Singapore, this course will provide an international forum for the exchange of information on materials and process characterization for semiconductor and integrated circuit technology with emphasis on diagnostics and control of materials and processes, failure and reliability analysis, and new analytical methods. The Shanghai location will provide good opportunities to establish contacts with a large number of scientists and technologies from the Pacific Rim and China.
[Contact: David G. Seiler, (301) 975-2054]

March 10-12, 1998 (San Diego, California)

Fourteenth Annual IEEE Semiconductor Thermal Measurement and Management Symposium (SEMI-THERM) 1998. Co-sponsored by NIST and IEEE, the symposium will present papers on current thermal management, modeling and measurement work on electronic components and systems in the following areas: thermal characterization - component through system; analytical and computational modeling and simulation; experimental methods and applications; thermal design and testing for reliability; and thermal aspects of high temperature electronics.
[Contact: David L. Blackburn, (301) 975-2068]

March 23-27, 1998 (Gaithersburg, Maryland)

1998 International Conference on Characterization and Metrology for ULSI Technology. The purpose of this workshop is to bring together scientists and engineers interested in all aspects of the technology and characterization techniques for semiconductor device research, development, manufacturing, and diagnostics: chemical and physical, electrical, optical, in-situ, and real-time control and monitoring.

The Workshop provides a forum to present and discuss critical issues; problems and limits; evolving requirements and analysis needs; future directions; and key measurement principles, capabilities, applications, and limitations. It will comprise of formal invited presentation sessions and poster sessions for contributed papers. The Workshop is the second in a series. The first was held at NIST January 30 to February 2, 1995. Papers from that Workshop were published in *Semiconductor Characterization: Present Status and Future Needs* (AIP Press, New York, 1996), W. M. Bullis, D. G. Seiler, and A. C. Diebold, editors. The Workshop is sponsored by NIST, Semiconductor Electronics Division, National Semiconductor Metrology Program, Electronics and Electrical Engineering Laboratory, SEMATECH, Semiconductor Research Corporation, American Vacuum Society - Manufacturing Science and Technology Division, and Semiconductor Equipment and Materials International (SEMI).
[Contact: David G. Seiler, (301) 975-2074]

EEEL Sponsors

National Institute of Standards and Technology
Executive Office of the President
U.S. Air Force
  Bolling Air Force Base; Newark Air Force Base; Patrick Air Force Base; CCG-Strategic Defense Command; CCG-Systems Command; Wright Patterson Air Force Headquarters, The Pentagon
U.S. Army
  Aberdeen Proving Ground; Redstone Arsenal
Department of Defense
  Advanced Research Projects Agency; Defense Nuclear Agency; Combined Army/Navy/Air Force (CCG); Information Systems Agency; National Security Agency
Department of Energy
  Basic Energy Sciences; Building Energy R&D; Energy Systems Research; Fusion Energy
Department of Justice
  Law Enforcement Assistance Administration
U.S. Navy
  CCG, Seal Beach; Naval Air Systems Command; Naval Research Laboratory; Naval Ordnance Systems Command; Naval Surface Warfare Center; Office of Naval Research
National Science Foundation
National Aeronautics and Space Administration
  NASA Headquarters; Langley Research Center; John F. Kennedy Space Flight Center
Department of Transportation
  National Highway Traffic Safety Administration

Environmental Protection Agency
MMIC Consortium
  Headquarters
  Various Federal Government Agencies
  Various Industry Companies
Scanning Capacitance Consortium
U.S. Japan Joint Optoelectronics Project
Delmarva Power
Nuclear Regulatory Commission
Pacific Gas and Electric
Sandia Labs
Tennessee Center for Research & Development
IMRA America, Inc.
Hughes Aircraft Co.
Honeywell, Inc.
Science Applications International, Inc.
Allied Signal Aerospace
Astralux, Inc.

NIST SILICON RESISTIVITY SRMs

The Semiconductor Electronics Division of NIST provides Standard Reference Materials (SRMs) for bulk silicon resistivity through the NIST Standard Reference Materials Program. An improved set of resistivity SRMs, on 100 mm wafers, will be available according to the schedule in the table below. These wafer SRMs improve upon the earlier 50 mm diameter SRM sets 1521, 1522, and 1523.

The new SRMs have similar values of nominal resistivity as the earlier set, but offer improved uniformity and substantially reduced uncertainty of certified values due both to material and procedural improvements. The most significant feature of the new SRMs is in their certification, which is performed using a dual-configuration four-probe measurement procedure rather than the single-configuration measurements specified in ASTM F84. Extensive testing has shown that the dual-configuration procedure reduces random variations of measurement and probe-to-probe differences.

Technical insights presented by the rigorous certification process are available in NIST Special Publication 260-131, *Standard Reference Materials:* The Certification of 100 mm Diameter Silicon Resistivity SRMs 2541 through 2547 Using Dual-Configuration Four-Point Probe Measurements. Individual data for each wafer are supplied along with the SRM certificate.

NIST SILICON BULK RESISTIVITY STANDARD REFERENCE MATERIALS

DATE UPDATED: 30 JUNE 1997

NOMINAL RESISTIVITY (ohm·cm)	NEW SRMs	AVAILABILITY
0.01	2541	NOW!
0.1	2542	NOW!
1	2543	end of CY 97
10	2541	10/1/97
25	2545	NOW!
100	2546	NOW!
200	2547	NOW!

NIST sells SRMs on an as-available basis. For technical information, contact James R. Ehrstein, (301) 975-2060; for ordering information, call the Standard Reference Materials Program Domestic Sales Office: (301) 975-6776.

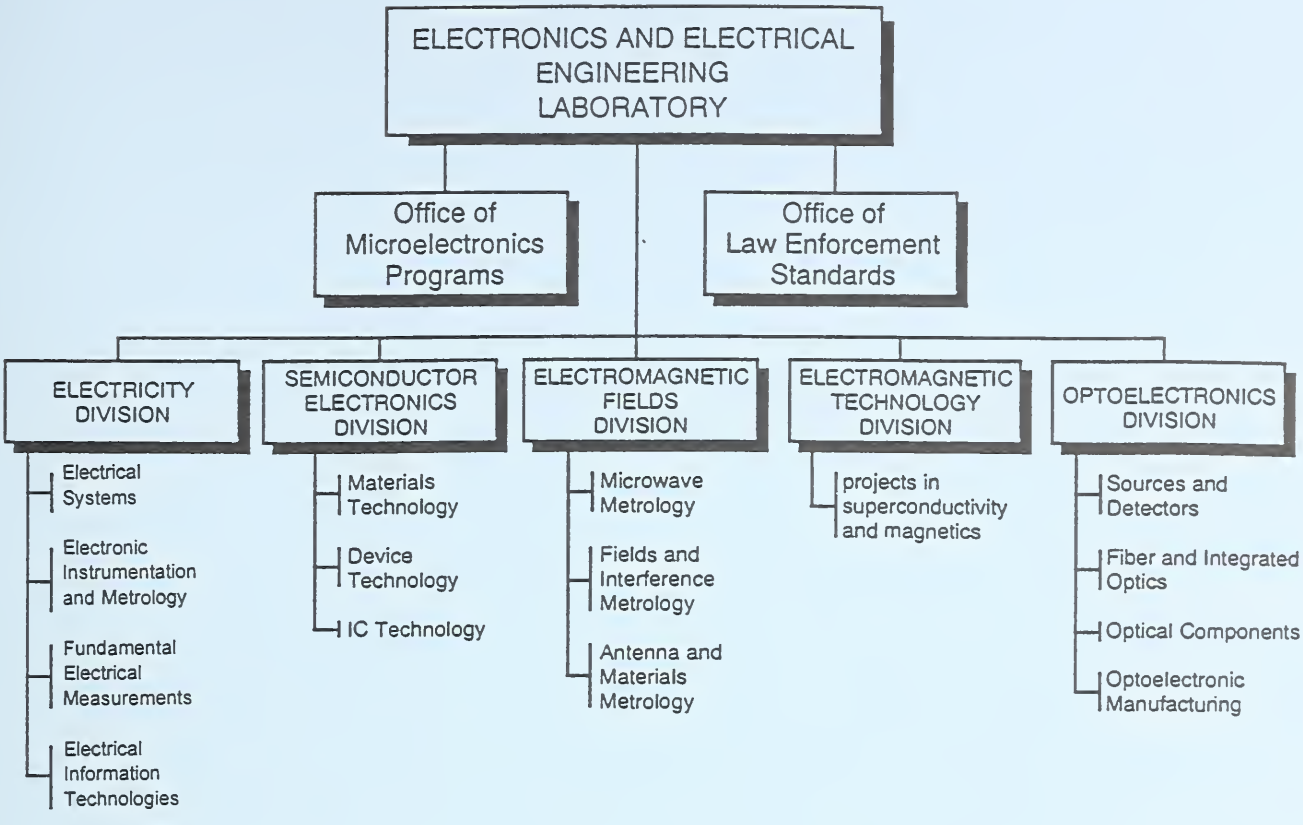

KEY CONTACTS

Laboratory Headquarters (810)	Director, Judson C. French (301) 975-2220
	Acting Deputy Director, Alan H. Cookson (301) 975-2220
	Acting Associate Director, Bruce F. Field (301) 975-2220
Office of Microelectronics Programs	Director, Robert I. Scace (301) 975-4400
Office of Law Enforcement Standards	Director, Kathleen M. Higgins (301) 975-2757
Electricity Division (811)	Chief, William E. Anderson (301) 975-2400
Semiconductor Electronics Division (812)	Chief, David G. Seiler (301) 975-2054
Electromagnetic Fields Division (813)	Chief, Allen C. Newell (303) 497-3131
Electromagnetic Technology Division (814)	Chief, Richard E. Harris (303) 497-3776
Optoelectronics Division (815)	Chief, Gordon W. Day (303) 497-5204

INFORMATION:

For additional information on the Electronics and Electrical Engineering Laboratory, write or call:

Electronics and Electrical Engineering Laboratory
National Institute of Standards and Technology
Metrology Building, Room B-358
Gaithersburg, MD 20899
Telephone: (301) 975-2220

U.S. DEPARTMENT OF COMMERCE
NATIONAL INSTITUTE OF STANDARDS AND TECHNOLOGY
GAITHERSBURG, MD 20899-0001